



**Three-Dimensional Neutronics Analysis of the  
SOLASE-H Laser Reactor  
Fissile-Enrichment-Fuel-Factory**

**M.M.H. Ragheb, M.Z. Youssef, S.I. Abdel-Khalik, and  
C.W. Maynard**

**November 1978**

**UWFDM-266**

***FUSION TECHNOLOGY INSTITUTE  
UNIVERSITY OF WISCONSIN  
MADISON WISCONSIN***

**Three-Dimensional Neutronics Analysis of the  
SOLASE-H Laser Reactor  
Fissile-Enrichment-Fuel-Factory**

M.M.H. Ragheb, M.Z. Youssef, S.I.  
Abdel-Khalik, and C.W. Maynard

Fusion Technology Institute  
University of Wisconsin  
1500 Engineering Drive  
Madison, WI 53706

<http://fti.neep.wisc.edu>

November 1978

UWFDM-266

### "LEGAL NOTICE"

"This work was prepared by the University of Wisconsin as an account of work sponsored by the Electric Power Research Institute, Inc. ("EPRI"). Neither EPRI, members of EPRI, the University of Wisconsin, nor any person acting on behalf of either:

"a. Makes any warranty or representation, express or implied, with respect to the accuracy, completeness, or usefulness of the information contained in this report, or that the use of any information, apparatus, method, or process disclosed in this report may not infringe privately owned rights; or

"b. Assumes any liabilities with respect to the use of, or for damages resulting from the use of, any information, apparatus, method or process disclosed in this report."

## Table of Contents

	Page
Abstract	iii
Acknowledgement	iv
Figure Captions	v
List of Tables	vi
1. Introduction	1
2. Three-Dimensional Parametric Cell Calculations	4
2.1 Introduction	4
2.2 The Monte Carlo Calculational and Geometrical Models	8
2.3 Material Compositions and Cross Section Data	14
3. Discussion of Results	16
3.1 Fissile and Fusile Breeding	16
3.2 Spatial Distribution of Fissile Fuel Production	24
3.3 Economic Considerations	38
4. Conclusions and Recommendations	41
Appendix: One-Dimensional Discrete Ordinates and Monte Carlo Scoping Studies	43
References	47

### Abstract

Three-dimensional neutronics of the SOLASE-H laser-fusion fissile-enrichment-fuel-factory (FEFF) for enriching fission power reactors fuel assemblies are presented. A new concept in which Light Water Reactors<sup>1</sup>(LWRs)  $\text{ThO}_2$  fuel assemblies constitute a lattice configuration with Pb as a neutron multiplier surrounding the fertile fuel is investigated. Three-dimensional parametric cell calculations for three blanket designs as a function of the neutron multiplier to fuel volume ratio of the lattice ( $v_m/v_f$ ) show that it is possible in such a concept to increase the fissile nuclei production densities in the fertile fuel, compared to cases where a lattice configuration is not used. It is suggested that the whole surface of the reactor cavity be surrounded with the Pb neutron multiplier. This leads to shorter times to attain projected average fissile enrichments, using substantially smaller fuel inventories, at the expense of the total fissile fuel production. Severe nonuniformities and asymmetries in the spatial distribution of the fissile enrichment are detected. Suppression of these uniformities is thought to require elaborate blanket spectral shaping and on-line fuel irradiation and management programs.

The time in years to attain an average 3 percent enrichment in the fertile fuel, the estimated fissile production in metric tons, the fissile nuclei production per source neutron, and the tritium yield per source neutron are for a suggested blanket design: 1.17, 2.27, 0.464, and 1.11, respectively. If a lattice configuration is not used, and the neutron multiplier does not surround the whole reactor cavity, for a configuration suggested by one-dimensional scoping studies, these numbers are: 3.46, 2.33, 0.479, and 1.12. The former design is also associated with a 50% reduction in the fuel inventory compared to the latter.

### Acknowledgement

This research was partially supported by a grant from the Electric Power Research Institute (EPRI).

The constructive discussions of W.F. Vogelsang, R.W. Conn, G.A. Moses from the Department of Nuclear Engineering, the University of Wisconsin, are greatly appreciated. Computer scheduling by J. Shanak from the Madison Academic Computing Center, The University of Wisconsin, the manuscript preparation by Miss Gail Herrington, the drafting by Mrs. Helga Fack, and the work by Mr. Dennis Bruggink are greatly acknowledged.

### Figure Captions

- Fig. 1 Side and Top Views of Radial and Axial Blankets of Fissile Enrichment Fuel Factory.
- Fig. 2 Unit Cell Reactor Geometry Model - Top View.
- Fig. 3 Unit Cell Reactor Geometry Model - Isometric View.
- Fig. 4 Spatial Distribution of Enrichment for Different Moderator-Multiplier to Fuel Volume Ratios, Design I.
- Fig. 5 Spatial Distribution of Enrichment for Different Moderator-Multiplier to Fuel Volume Ratios, Design II.
- Fig. 6 Spatial Distribution of Enrichment for Different Moderator-Multiplier to Fuel Volume Ratios, Design III.
- Fig. 7 Fissile and Fusile Breeding as a Function of  $v_m/v_f$  for Designs I, II, and III.
- Fig. 8 Average Fissile Production and Fissile Production Density as a Function of  $v_m/v_f$  for Designs I, II, and III.
- Fig. A.1 The Comparative Discrete-Ordinates and Monte Carlo One-Dimensional Geometry Model of the Fissile Enrichment Fuel Factory.

### List of Tables

Table I	Elemental Compositions of Material Mixes.
Table II	Group Structure, Average Number of Neutrons Released Per Fission and Fission Spectrum.
Table III	Breeding in Fissile Enrichment Fuel Factory as a Function of $v_m/v_f$ (Nuclei/Source Neutron), Design I.
Table IV	Breeding in Fissile Enrichment Fuel Factory as a Function of $v_m/v_f$ (Nuclei/Source Neutron), Design II.
Table V	Breeding in Fissile Enrichment Fuel Factory as a Function of $v_m/v_f$ (Nuclei/Source Neutron), Design III.
Table VI	Average Breeding Densities in Fissile Enrichment Fuel Factory as a Function of $v_m/v_f$ (Nuclei/Source Neutron $\cdot \text{cm}^3$ of Breeding Zone), Design I.
Table VII	Average Breeding Densities in Fissile Enrichment Fuel Factory as a Function of $v_m/v_f$ (Nuclei/Source Neutron $\cdot \text{cm}^3$ of Breeding Zone), Design II.
Table VIII	Average Breeding Densities in Fissile Enrichment Fuel Factory as a Function of $v_m/v_f$ (Nuclei/Source Neutron $\cdot \text{cm}^3$ of Breeding Zone), Design III.
Table IX	$\text{Th}(n,\gamma)$ Reaction (Nuclei/Source Neutron) in Fissile Enrichment Fuel Factory in Different Radial Blanket Parts as a Function of $v_m/v_f$ , Design I.
Table X	$\text{Th}(n,\gamma)$ Reaction (Nuclei/Source Neutron) in Fissile Enrichment Fuel Factory in Different Radial Blanket Parts as a Function of $v_m/v_f$ , Design II.
Table XI	$\text{Th}(n,\gamma)$ Reaction (Nuclei/Source Neutron) in Fissile Enrichment Fuel Factory in Different Radial Blanket Parts as a Function of $v_m/v_f$ , Design III.
Table XII	Tritium Breeding in Different Parts of Radial Blanket (Nuclei/Source Neutron) of Fissile Enrichment Fuel Factory as a Function of $v_m/v_f$ , Design I.
Table XIII	Tritium Breeding in Different Parts of Radial Blanket (Nuclei/Source Neutron) of Fissile Enrichment Fuel Factory as a Function of $v_m/v_f$ , Design II.
Table XIV	Tritium Breeding in Different Parts of Radial Blanket (Nuclei/Source Neutron) of Fissile Enrichment Fuel Factory as a Function of $v_m/v_f$ , Design III.



Table XV	Economic Parameters for Fissile Enrichment Fuel Factory as a Function of $v_m/v_f$ for Designs I, II and III.
Table A.1	Comparison of Different One-Dimensional Blanket Compositions and Configurations With Respect to Breeding.

## 1. Introduction

Multi-dimensional neutronics analyses using Monte Carlo for the SOLASE-H<sup>(1)</sup> Laser-Fusion Fissile-Enrichment-Fuel-Factory (FEFF) for enriching fission power reactor fuel assemblies are presented. Proliferation concerns have recently aroused interest in thorium-containing fuel cycles. Moreover,  $^{233}\text{U}$  produced from  $^{232}\text{Th}$  is a better performer in Light Water Reactors (LWRs) than Pu. In a Fusion Fuel Factory (FFF), as discussed by Bethe<sup>(2)</sup>, it is thought that the copious presence of gamma-active isotopes is a safeguard against diversion for weapons manufacture during fuel reprocessing, and denaturing or spiking may be unnecessary.<sup>(2)</sup> Results of neutronics analyses of the concept of a Laser-Fusion FEFF are presented in which LWRs thorium oxide<sup>(1,3)</sup> fresh-fuel assemblies are enriched in  $^{233}\text{U}$  before shipment to a LWR. Such a concept offers potentially tighter proliferation control by eliminating the reprocessing and refabrication stages. Alternatively, reprocessing may be carried out within safeguarded fuel production reprocessing centers. It can also be easily integrated into the existing LWR economy.

The objective of our study was to attain neutronically optimized designs which will maximize fissile fuel production, give a tritium breeding ratio around unity to make the FEFF self-sustaining, and minimize both the fuel inventory and the residence time of the fuel assemblies in the FEFF. The performance of three studied designs is exposed in this work. A concept is introduced in which the fuel assemblies constitute a lattice configuration with Pb as a neutron multiplier surrounding the fertile fuel.

Parametric three-dimensional cell calculations as a function of the neutron multiplier-moderator to fuel volume ratio of the lattice ( $v_m/v_f$ ) show that it is possible in such a concept to enhance breeding densities in the fertile fuel. This leads to shorter times to attain projected average enrichments in  $^{233}\text{U}$  in the fuel assemblies, using substantially smaller fuel inventories at the expense of a reduction in the yearly fissile production. The shorter times to attain a certain enrichment and the reduced fuel inventories may have favorable safety and economical implications. Including a neutron multiplier zone in the axial blanket is found to substantially increase the fissile breeding in the radial blanket, at the expense of a reduction of tritium breeding in the axial blanket. It is established that the neutronic coupling between the radial and axial blankets questions the validity of simple solid angle weightings adopted in previous studies. Severe nonuniformities and asymmetries in the spatial distribution of the fissile enrichment radially and axially are detected. They are caused by the reactor geometry as a right-circular-cylinder blanket, surrounding the point fusion source at its center. Suppression of these nonuniformities will necessitate elaborate blanket spectral shaping and on-line fuel irradiation and management programs.

Symbiotic and hybrid fission-fusion reactors may be considered as a third nuclear energy alternative in the future, pure fusion and the fast fission breeder being the two other alternatives. A crucial necessity for the introduction of such energy options is the increasingly threatening shortage in the supply of  $^{235}\text{U}$  which is the only naturally-existing fissile isotope,<sup>(5)</sup> and the expected, not so-well publicized, environmentally deleterious consequences of a coal-based economy.<sup>(6)</sup> The coupling

between fission and fusion has been addressed by various researchers.<sup>(1-3,16)</sup> Their integration relies on the fact that fission reactors are "power-rich" releasing an energy of 200 MeV/fission event compared to 17.6 MeV/fusion event, but "neutron-poor" releasing 2 MeV low-energy fission neutrons, compared to 14.06 MeV high-energy fusion D-T neutrons. The coupling of both systems in a certain way may thus be more optimal than either one independently. Sub-Lawson plasma confinement parameters in magnetic confinement fusion, and low laser/electron/ion beam conversion efficiencies in inertial confinement, may thus be tolerated, because of the possible fissile fuel production and the neutron multiplication with high energy fusion neutrons. It can thus be expected that it will be possible for fission-fusion reactors to have an earlier introduction into the economy than pure fusion devices, possibly also opening the way for them. If the fast fission breeder technology is judged too dangerous or expensive, fission-fusion symbiotic systems may prove very attractive, especially if  $^{233}\text{U}$  is the fissile nuclide produced, because of its high thermal generation factor  $\eta$ . In this case, the existing LWR technology will be supplied with its need in fissile fuel. The possibility of enriching fuel in a fusion reactor for shipment to a fission reactor was discussed by Conn, et al.<sup>(1,2)</sup> and by Rozhkov and Shatalov.<sup>(14)</sup> The non-proliferation aspects of such a concept which eliminates the weak link of reprocessing and refabrication have been discussed by Conn, et al.<sup>(1,2,16)</sup> as well as by Bethe,<sup>(2)</sup> the latter with the reprocessing stage included. In a scheme similar to the one suggested by Feiveson, Taylor, von Hippel and Williams for fast breeders,<sup>(18)</sup> the FEF, as considered in

the present study, would be under international control (e.g. the International Atomic Energy Agency: IAEA), and the converter reactors using the produced  $^{233}\text{U}$  would be available to countries and organizations that need them.

In Sec. 2, the parametric three-dimensional cell calculations, and the Monte Carlo models for three basic designs denoted as Design I, II and III, are exposed. Results of the computations are discussed in Sec. 3. An appendix includes comparative one-dimensional Monte Carlo and discrete ordinates scoping studies. Conclusions from the present study are summarized in Sec. 4.

## 2. Three-Dimensional Parametric Cell Calculations

### 2.1. Introduction

The considered reactor geometry is shown in Fig. 1. Three LWR fuel assemblies of 4 m length each are placed on top of each other and surround as a radial cylindrical blanket the point 14.06 MeV neutron source resulting from the laser-induced fusion reactions at the center of the cavity of 6 m radius and 12 m height. An axial blanket is emplaced at the top and bottom of the radial blanket, and is used solely for fusile breeding. A stainless steel structure is used. A 67% C-33 v/o Pb mixture is used as a reflector-shield for both the radial and axial blankets. Pb canned in Zircaloy-2 and cooled by Na is used as a neutron multiplier. Pb was preferred to Be since it does not pose toxicity and availability problems, and leads to a harder spectrum in the blanket. This will reduce the fissioning of the produced  $^{233}\text{U}$  with thermal neutrons. In the radial blanket, a Pb zone faces the 14.06 MeV neutron flux to take advantage of the threshold  $\text{Pb}(n,2n)$  reaction for the three considered designs I, II, and III. Only in design III, it also faces the neutron source in the axial blanket.

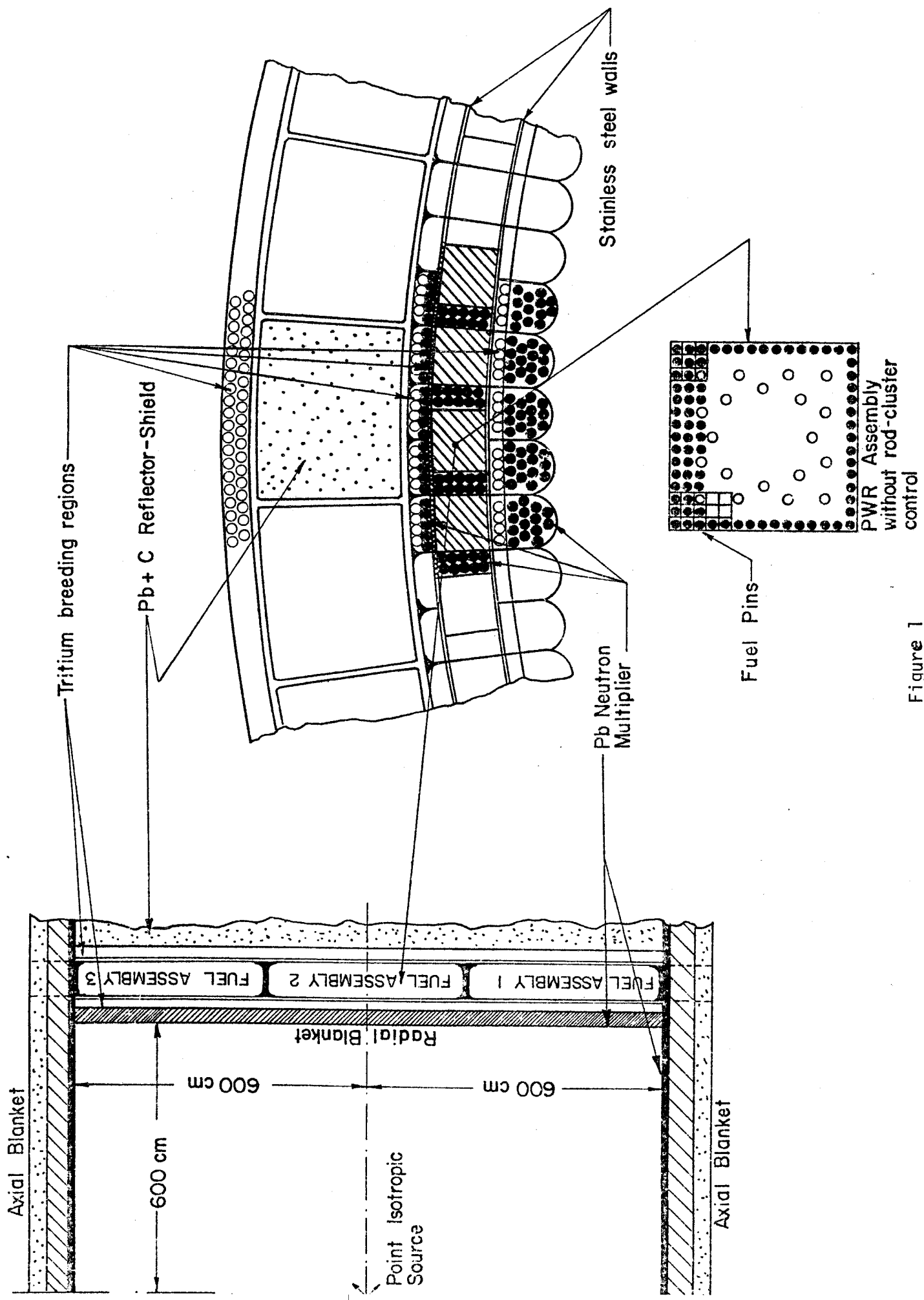


Figure 1

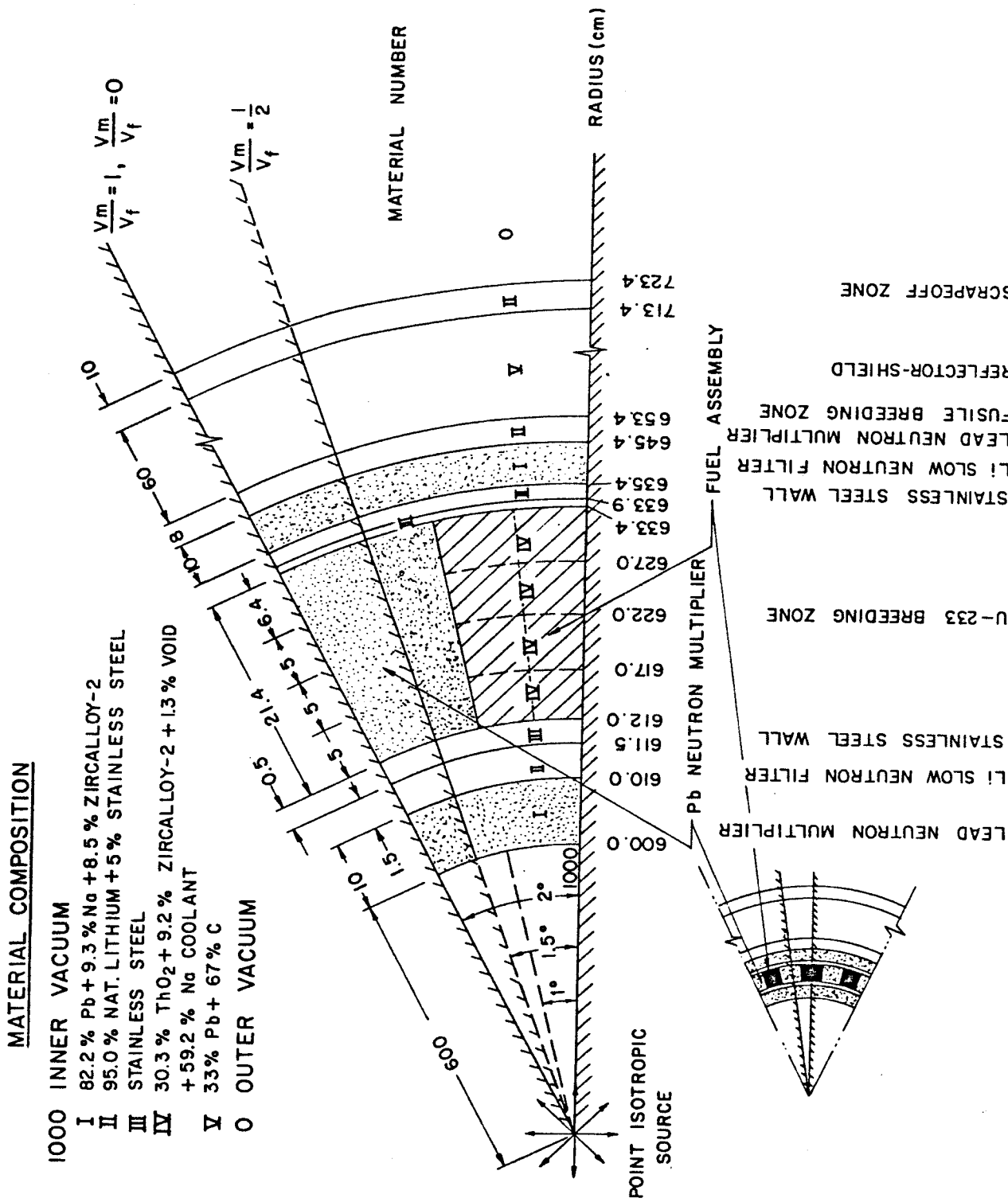
In the radial blanket the first Pb layer is followed by a thin layer of natural lithium canned in stainless steel, which filters slow neutrons and prevents them from reaching the next zone containing the  $\text{ThO}_2$ , Zircaloy-2 clad, and Na-cooled fuel assemblies. Filtering of the slow neutrons is beneficial for tritium breeding and for avoidance of the fissioning of the bred  $^{233}\text{U}$ . Another thin region of Li follows the fissile breeding region to filter the slow neutron flux component reflected from the reflector. This filtering effect has another beneficial effect in that it prevents the formation of the U-233 in the outer layers of the fuel subassemblies, since the  $\text{Th-232} (n, \gamma) \text{U-233}$  reaction behaves in a  $1/v$  manner. This will otherwise lead to a nonuniform enrichment of the fuel, resulting in turn in nonuniform power generation when the fuel subassemblies are later used in LWRs. A third fissile breeding scrapeoff zone follows the reflector in the radial blanket to intercept leaking neutrons, and is followed by the biological shield. In preliminary studies, the fuel assemblies were emplaced next to each other. This entailed a rather large fuel inventory, and a long time to attain an average enrichment of the irradiated fuel. It was reasoned that since the neutron source in the system is constant, reducing the fertile fuel inventory would lead to higher fissile breeding densities and subsequent shorter times to attain a required fissile enrichment. This could have been obviously achieved by reducing the system size, but was precluded by radiation damage considerations to the first wall. A  $2 \text{ MW/m}^2$  14.06 MeV neutron first wall loading is considered at the center of the cavity of radius 6 m. The total 14.06 MeV neutron power of the reactor is thus:

$$2 \left( \frac{\text{MW}}{\text{m}^2} \right) \cdot 4 \cdot \pi \cdot 6^2 (\text{m}^2) = 9.048 \times 10^2 (\text{MW}) .$$

Being compelled to keep the reactor dimensions unchanged from the point of view of the mechanical heat transfer and materials designs, the reduced amount of fuel had to be replaced by a material which will scatter the neutrons azimuthally into the fuel subassemblies, with minimal absorption, so that the neutron economy would not be much hindered. Pb was chosen for this purpose, due to its added advantage as a neutron multiplier. It will also not thermalize the spectrum, which is required to remain a hard one to avoid excessive fissioning of the bred U-233. A lattice configuration was chosen with the Pb neutron multiplier/moderator surrounding the fuel subassemblies as shown in Fig. 2. In Design I, the fuel zone is followed by a Li zone preceding the reflector in the radial blanket, whereas in Designs II and III this Li zone is preceded by a Pb zone. A three-dimensional study was needed to investigate the suggested concept of a lattice configuration, which cannot be achieved by either one or two-dimensional models. Moreover, in a related study of a magnetically-protected first wall laser driven reactor, Ragheb, Cheng and Conn<sup>(21)</sup> reported severe asymmetry effects in the axial direction caused by the source-reactor geometry, and the magnitude of this effect needed to be studied in the considered design. Comparative discrete ordinates and Monte Carlo one-dimensional scoping studies are exposed in the appendix. We point out the inadequacy of one-dimensional models for such studies, since they over estimate their breeding capabilities. Severe inhomogeneities in fissile production are detected in the axial and radial directions.



## Figure 2



The suggested lattice configuration achieves its intended purpose of increased breeding densities and resulting shorter enrichment times. A parametric study is carried with respect to  $v_m/v_f$ , the multiplier-moderator to fuel volume ratio. The calculational models used in the investigation are described in the next subsections.

## 2.2 The Monte-Carlo Calculational and Geometrical Models

The total 14.06 MeV FEFf fusion power of  $9.048 \times 10^2$  MW corresponds to the following isotropic neutron source at the center of the reactor cavity:

$$S_n = 9.048 \times 10^2 \text{ (MW)} \times 10^6 \text{ (w)} \times \frac{1}{1.6021 \times 10^{-13} \text{ (MeV/sec)}} \cdot \frac{1}{14.1 \text{ (MeV)}}$$

$$= 4.005 \times 10^{20} \left( \frac{14.1 \text{ MeV Source Neutrons}}{\text{sec}} \right) .$$

Because of symmetry, only the upper part of the reactor is considered. This upper part is now divided into three regions of 200 cm each in the axial direction denoted as: central part of radial blanket, middle part of radial blanket, and upper part of radial blanket. Each part is then divided into several radial regions. For consideration of the cell calculations "pie-slice" configurations were considered corresponding to different multiplier-moderator to fuel volume ratios as shown in Figs. 2 and 3. Radially, each axial region is divided into several sub-regions: a Pb multiplier zone (10 cm) followed by a fusile breeding zone (1.5 cm), then by a fissile breeding zone (21.4 cm). The fissile breeding zone is enclosed within two 0.5 cm thick stainless steel walls. Adjacent to the fuel zone is the neutron multiplier/moderator zone. Different

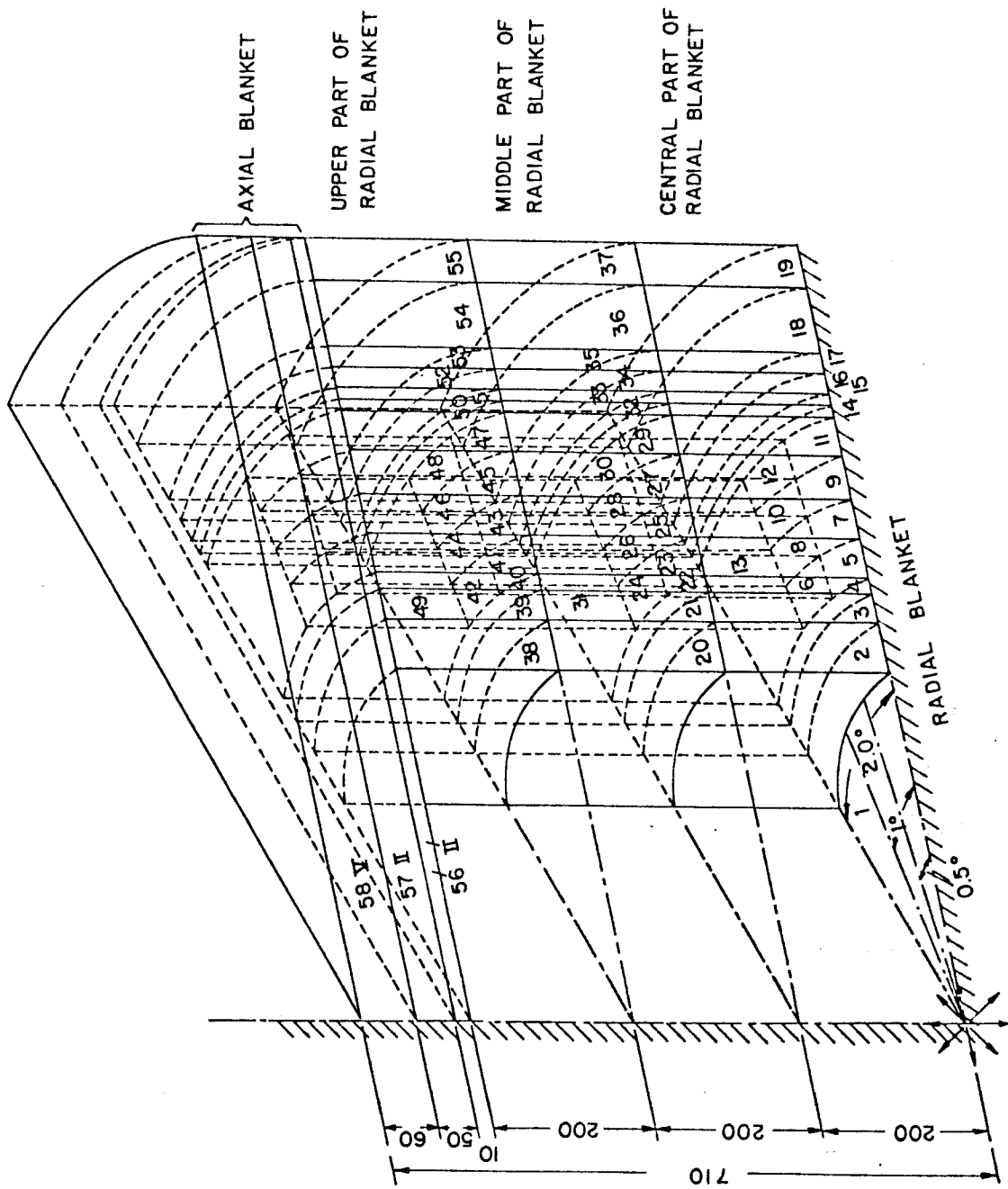


Figure 3

considered  $v_m/v_f$  ratios correspond to different azimuthal angles for the "pie-slice". Values of  $v_m/v_f = 1/2, 1, 0$  correspond of azimuthal angles for the unit cell of  $1.25^\circ$ ,  $1.5^\circ$  and  $2^\circ$ , respectively. For the last case ( $v_m/v_f = 1$ ), the Pb zone adjacent to the fertile fuel zone is replaced by fuel in the numerical simulations. Notice that the top views in Figs. 2 and 3 represent half a unit cell because of the azimuthal symmetry of the unit cells.

In Design I the fissile breeding zone is followed by an 8 cm thick fusile breeding zone, then by the reflector and a scrapeoff Li zone. Based on the results of a one-dimensional parametric study as shown in Table A.1 in the appendix, Designs II and III differ from Design I in the inclusion of a 1.5 cm Li filtering zone followed by a 10 cm thick Pb neutron multiplying zone before an 8 cm fusile breeding zone directly preceding the reflector. To investigate the radial distribution of the quantities of interest, the fissile breeding zone was subdivided into 4 radial regions of 5, 5, 5 and 6.4 cm, respectively. In Design III the axial blanket is composed of a 10 cm Pb neutron multiplying zone, followed by a 50 cm natural Li blanket and a 60 cm reflector. In Designs I and II, no neutron multiplier zone was used. Instead, a 60 cm thick blanket followed by a 60 cm reflector were used.

The neutron source was sampled isotropically within the discussed geometry. The polar angle  $\theta$  was sampled according to:

$$P(\theta) = \frac{\int_0^\alpha \int_0^\theta \sin\theta' d\theta' d\psi}{\int_0^\alpha \int_0^{\pi/2} \sin\theta' d\theta' d\psi} = 1 - \cos\theta .$$

The azimuthal angle  $\psi$  was sampled uniformly from 0 to  $\alpha$  to correspond to different cell configurations for  $v_m/v_f$ , keeping the volume of the fissile breeding zone constant. The sampled  $\theta$  and  $\psi$  were used to obtain direction cosines for the isotropic source within the considered solid angles.

The MORSE Monte Carlo code<sup>(22,23,24)</sup> was used in the calculations. However, the RSIC-communicated version<sup>(23)</sup> does not treat external source-driven multiplying media. Modifications for treating the continuous slowing down of the 14.06 MeV fusion neutrons in multiplying media with statistical weighting were implemented. Details of the methodology adopted is reported elsewhere.<sup>(31)</sup> The energy group structure adopted as well as the corresponding values of the average number of neutrons released per fission event ( $\nu$ ) are shown in Table II. The values of  $\nu$  in Table II are average flat-weighted energy group values using the relationship:

$$\nu(\Delta E) = \frac{\int_{E_{\text{lower}}}^{E_{\text{upper}}} \nu(E) dE}{\int_{E_{\text{lower}}}^{E_{\text{upper}}} dE}$$

where:  $E_{\text{upper}}$ ,  $E_{\text{lower}}$  are the upper and lower group boundaries (MeV), respectively, and:  $\nu(E) = 2.047 + 0.153E$  for Th-232. Notice that the constants reported in Lamarsh<sup>(33)</sup> seem to be in error.

The multiplication-weighting method reported in Ref. 31 was used in this work.

The formula for the fission spectrum used was the one determined by Watt<sup>(25)</sup>:

$$N(E) = 0.484 \sinh \sqrt{2E} e^{-E}$$

Table I Elemental Compositions of Material Mixes

Material Composition	Elements	Nuclei Densities Nuclei/(barn.cm)
Neutron Multiplication Zones 82.2 v/o Pb + 9.3 v/o Na + 8.5 v/o Zircaloy-2	Ni Cr Fe Pb Na Zr Sn	.18314-5 .32965-5 .43953-5 .25345-1 .23657-2 .35983-2 .54941-4
Fusile Breeding Zones 95 v/o Natural Lithium + 5 v/o Stainless Steel	Ni Cr Fe Li-6 Li-7	.46900-3 .72500-3 .30705-2 .31514-2 .39321-1
Stainless Steel Structure	Ni Cr Fe	.93800-2 .14500-1 .61400-1
Fissile Breeding Zones 30.3 v/o ThO <sub>2</sub> + 9.2 v/o Zircaloy-2 +1.3 v/o Void + 59.2 v/o Na Coolant	Ni Cr Fe O Na Zr Sn Th	.19929-5 .35872-5 .47829-5 .13871-1 .15032-1 .39156-2 .59786-4 .69353-2
Reflector-Shield 33 v/o Pb + 67 v/o C	C Pb	.53487-1 .11161-1

where:  $N(E)$  is the fraction of neutrons emitted per fission with an energy  $E$ , in MeV, per unit energy range. This formula is regarded as adequate for the energy range 0.075 to 17 MeV. Group values were deduced according to:

$$N(E) = \frac{\int_{E_{\text{lower}}}^{E_{\text{upper}}} N(E) dE}{\int_{E_{\text{lower}}}^{E_{\text{upper}}} dE}$$

### 2.3 Material Compositions and Cross-Section Data

The material compositions considered, and the corresponding nuclei densities are shown in Table I. For the fuel assemblies, these correspond to a standard PWR assembly with an array of 17 x 17 fuel pins, and 21.4 cm side-length. Each subassembly contains 264 fuel elements of 0.9498 cm outer diameter and an 1.25 cm square pitch. The cladding is Zircaloy-2 of 0.0572 cm thickness. Fuel pellet diameters are thus 0.819 cm. Twenty-five locations for the control rod clusters when used in a LWR are present, but are not used. The fuel breeding zone consists of a single row of fuel assemblies, interspersed with regions of Pb neutron multiplier/moderator. To provide efficient cooling, both the neutron multiplying and the fissile breeding zones are cooled with Na, but will be water-cooled when used in a LWR. In the fissile breeding zone natural lithium was used for fissile breeding, and leads to acceptable fissile breeding. Higher fissile breeding

Table II      Group Structure, Average Number of Neutrons  
Released Per Fission and Fission Spectrum.

Group	Upper Edge (eV)	Average Number of Neutrons Released Per Fission	Fission Spectrum for Th-232
1	1.4918+7	4.221	4.13402-5
2	1.3499+7	4.014	1.13716-4
3	1.2214+7	3.827	2.77726-4
4	1.1052+7	3.657	6.10852-4
5	1.0000+7	3.504	1.22033-3
6	9.0484+6	3.366	2.23789-3
7	8.1873+6	3.240	3.79806-3
8	7.4082+6	3.127	6.01365-3
9	6.7032+6	3.024	8.94399-3
10	6.0653+6	2.931	1.25756-2
11	5.4881+6	2.811	3.82868-2
12	4.4933+6	2.672	5.75022-2
13	3.6788+6	2.559	7.53082-2
14	3.0119+6	2.466	8.82827-2
15	2.4660+6	2.339	2.78442-1
16	1.3534+6	2.207	2.08445-1
17	7.4274+5	2.135	1.17664-1
18	4.0762+5	2.091	7.25101-2
19	1.6473+5	2.062	2.63308-2
20	3.1828+4	2.050	2.47411-3
21	3.3546+3	2.047	8.56395-5
22	3.5358+2	2.047	2.93411-6
23	3.7267+1	2.047	1.00411-7
24	3.9279+0	2.047	3.43606-9
25	4.1400-1	2.047	1.20247-10

Lower Edge: 1.0000-4



values can be obtained by breeding part of the tritium in the fed LWRs, using a higher Li-density material such as  $\text{Li}_2\text{O}$ , or slightly enriching the Li in the Li-6 isotope. The reflector is a mixture of Pb and C to act as a primary gamma shield on the one hand, and slow down the leaking fast neutrons by radiative capture reactions, on the other.

The transport cross-sections were taken from the coupled 100 n-21  $\gamma$  group cross section library prepared for EPR calculations by Plaster, Santoro, Roussin and Ford III<sup>(26,27)</sup> and designated as DLC-37B by the Radiation Shielding Information Center.<sup>(28)</sup> These were compiled from the ENDF/B-IV data file. A group-collapsed set in the structure shown in Table II was used, keeping the GAM-II<sup>(29)</sup> structure for the top six groups.

Reaction cross sections were used as group-collapsed data from the work of Abdou and Roussin.<sup>(30)</sup>

Results of computations are discussed in the next section.

### 3. Discussion of Results

#### 3.1 Fissile and Fusile Breeding

Tables III, IV and V show a summary for the fusile and fissile breeding in the suggested Designs I, II and III, respectively. It should be remembered that Designs II and III have a Pb zone between the fissile breeding zone and the reflector so that the fertile fuel is surrounded by Pb in a flux trap, whereas Design I has only a fusile breeding zone at this location. A Pb multiplier zone also precedes the axial blanket in Design III. For the cases where the suggested lattice configuration is not used ( $v_m/v_f = 0$ ) one obtains a  $\text{Th}(n,\gamma)$  reaction per source neutron of 0.479, 0.504 and 0.613 for

Table III Breeding in Fissile Enrichment Fuel Factory as a  
Function of  $v_m/v_f$  (Nuclei/Source Neutron) Design I

$v_m/v_f$	Th(n, $\gamma$ )	T6 <sup>+</sup>		T7		T6 + T7 Axial and Radial Blankets	T6 + T7 + Th(n, $\gamma$ )
		Radial Blanket	Axial Blanket	Radial Blanket	Axial Blanket		
0	4.79-1+1.15-2	3.20-1+1.13-2	5.82-1+1.06-2	2.44-2+2.62-3	1.94-1+8.05-3	1.12+0+1.77-2	1.60+0+2.11-2
1/2	3.93-1+7.99-3	3.80-1+1.39-2	6.26-1+1.29-2	1.79-2+1.89-3	1.96-1+7.50-3	1.22+0+2.05-2	1.61+0+2.20-2
1	3.40-1+7.85-3	4.22-1+1.58-2	6.29-1+1.62-2	2.04-2+2.49-3	2.06-1+6.22-3	1.28+0+2.36-2	1.62+0+2.49-2

<sup>+</sup>T6 and T7 are tritium yields from reactions with <sup>6</sup>Li and <sup>7</sup>Li, respectively

Table IV Breeding in Fissile Enrichment Fuel Factory as a  
Function of  $v_m/v_f$  (Nuclei/Source Neutron) Design II

$v_m/v_f$	Th(n, $\gamma$ )	T6 <sup>+</sup>		T7		T6 + T7 Axial and Radial Blanket	T6 + T7 + Th(n, $\gamma$ )
		Radial Blanket	Axial Blanket	Radial Blanket	Axial Blanket		
0	5.04-1+1.24-2	3.18-1+1.23-2	5.74-1+1.19-2	1.96-2+2.15-3	1.80-1+7.48-3	1.09+0+1.88-2	1.59+0+2.25-2
1/2	4.23-1+8.32-3	3.45-1+1.18-2	6.45-1+1.10-2	1.11-2+1.34-3	1.90-1+9.76-3	1.19+0+1.89-2	1.61+0+2.07-2
1	3.56-1+7.29-3	3.90-1+1.35-2	6.35-1+1.08-2	1.60-2+1.70-3	1.94-1+7.14-3	1.24+0+1.88-2	1.60+0+2.02-2

+ T6 and T7 are tritium yields from reactions with  ${}^6\text{Li}$  and  ${}^7\text{Li}$ , respectively

Table V Breeding in Fissile Enrichment Fuel Factory as a  
Function of  $v_m/v_f$  (Nuclei/Source Neutron) Design III

$v_m/v_f$	Th(n, $\gamma$ )	T6 <sup>+</sup>		T7		T6 + T7 Axial and Radial Blanket	T6 + T7 + Th(n, $\gamma$ )
		Radial Blanket	Axial Blanket	Radial Blanket	Axial Blanket		
0	6.13-1+1.53-2	3.29-1+1.26-2	5.37-1+2.00-2	1.17-2+1.51-3	6.73-2+6.26-3	9.45-1+2.45-2	1.56+0+2.89-2
1/2	5.31-1+9.31-3	4.10-1+1.33-2	5.63-1+1.16-2	1.59-2+2.07-3	7.15-2+6.48-3	1.06+0+1.89-2	1.59+0+2.11-2
1	4.64-1+8.58-3	4.81-1+1.55-2	5.45-1+1.53-2	1.34-2+1.77-3	7.02-2+5.31-3	1.11+0+2.25-2	1.57+0+2.41-2

+ T6 and T7 are tritium yields from reactions with  ${}^6\text{Li}$  and  ${}^7\text{Li}$ , respectively

Designs I, II, and III, respectively. The corresponding tritium productions per source neutron are 1.12, 1.09 and 0.945. Lattice configurations for  $v_m/v_f = 0, 1/2, 1$  were investigated for the three designs. The fusile breeding increases for higher values of  $v_m/v_f$ , whereas the fissile breeding goes down. The decrease in Design III is slower than in Design I. In the last column of Tables III, IV and V the sum of the fusile and fissile breeding seems to remain almost constant for either design. In all cases the axial blanket contributes more to the tritium production than the radial blanket, mostly from reactions with Li-6. The addition of the 10 cm Pb zone before the reflector in Design III improved the fissile breeding in the radial blanket substantially and is recommended as a design feature. However, the addition of the neutron multiplying zone in Design III in front of the axial blanket did not help in increasing the fusile breeding in the axial blanket. As a matter of fact, it decreases the breeding from the Li-7 isotope.

The results show that the tritium breeding in the axial blanket is a function of the  $v_m/v_f$  ratio in the radial blanket. Thus, the two blankets are closely coupled neutronically. One-dimensional models using simple solid angle weightings<sup>(11)</sup> are thus judged inadequate for such systems, since they cannot take into consideration this coupling effect.

Tables VI, VII and VIII display the breeding densities of fusile and fissile fuel production defined as:

$$\text{Breeding Density} = \frac{\text{Number of fusile or fissile nuclei produced per 14.06 MeV Source Particle}}{\text{Total Volume of Breeding Zone in cm}^3} .$$

Table VI      Average Breeding Densities in Fissile Enrichment  
 Fuel Factory as a Function of  $v_m/v_f$  (Nuclei/Source  
 Neutron  $\cdot$  cm<sup>3</sup> of Breeding Zone) Design I

$v_m/v_f$	Th(n, $\gamma$ )	<sup>6</sup> Li(n, $\alpha$ )T		<sup>7</sup> Li(n,n' $\alpha$ )T		Total Tritium Production Density
		Radial Blanket	Axial Blanket	Radial Blanket	Axial Blanket	
0	4.77-9	3.19-9	2.95-9	2.44-10	9.83-10	3.76-9
1/2	5.87-9	3.89-9	3.17-9	1.79-10	9.93-10	4.10-9
1	6.77-9	4.21-9	3.19-9	2.04-10	1.04-09	4.30-9

Table VII Average Breeding Densities in Fissile Enrichment  
 Fuel Factory as a Function of  $v_m/v_f$  (Nuclei/Source  
 Neutron  $\cdot$  cm<sup>3</sup> of Breeding Zone) Design II

$v_m/v_f$	Th(n, $\gamma$ )	${}^6\text{Li}(n,\alpha)\text{T}$		${}^7\text{Li}(n,n'\alpha)\text{T}$		Total Tritium Production Density
		Radial Blanket	Axial Blanket	Radial Blanket	Axial Blanket	
0	5.01-9	2.96-9	3.49-9	1.82-10	1.09-9	4.01-9
1/2	6.32-9	3.21-9	3.92-9	1.03-10	1.16-9	4.83-9
1	7.08-9	3.63-9	3.86-9	1.49-10	1.18-9	4.56-9

Table VIII Average Breeding Densities in Fissile Enrichment  
 Fuel Factory as a Function of  $v_m/v_f$  (Nuclei/Source  
 Neutron  $\cdot \text{cm}^3$  of Breeding Zone) Design III

$v_m/v_f$	$\text{Th}(n, \gamma)$	${}^6\text{Li}(n, \alpha)\text{T}$		${}^7\text{Li}(n, n'\alpha)\text{T}$		Total Tritium Production Density
		Radial Blanket	Axial Blanket	Radial Blanket	Axial Blanket	
0	6.10-9	3.06-9	3.27-9	1.09-10	4.09-10	3.48-9
1/2	7.93-9	3.82-9	3.42-9	1.48-10	4.35-10	3.90-9
1	9.23-9	4.48-9	3.32-9	1.25-10	4.27-10	4.08-9

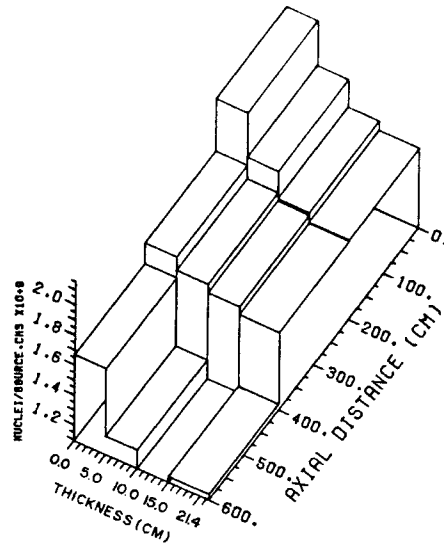


These values have a one-to-one correspondence to those in Tables III, IV and V. Now, the fissile breeding densities increase with increasing values of  $v_m/v_f$ . The increase is much more pronounced in Design III than in Designs I and II. Note that increased values of the breeding densities mean shorter times to attain a required average fuel enrichment, using a smaller fertile inventory. This is the major merit of using a Pb multiplier in front of the axial blanket and a lattice configuration in which Pb surrounds the fertile fuel. A simplified economic analysis will be presented in Sec. 3.3. In the next section we investigate the spatial distribution of fissile production.

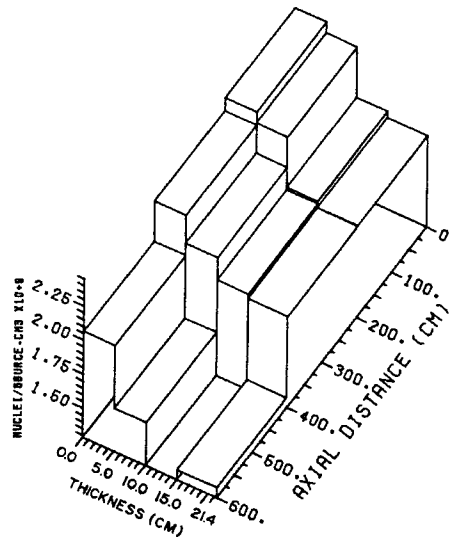
### 3.2 Spatial Distribution of Fissile Fuel Production

Severe spatial nonuniformities in the fissile fuel production are detected in all cases. Figs. 4, 5, 6 show the distribution of fuel production per source neutron in the fuel assemblies both radially and axially for Designs I, II and III. These figures reveal that the  $\text{Th}(n,\gamma)$  reaction rate per source neutron is steep near the front edge of the fuel assemblies facing the plasma, especially around the center of the reactor cavity. This will result in severe metallurgical and heat transfer problems when operated in the LWRs, resulting in uneven burnup of the fuel. However, the bred  $^{233}\text{U}$  in the outer layer of the assemblies will also be burned in situ faster than what is burnt in the inner layers. Thus, these two balancing effects may cancel each other, and no general conclusions can be drawn without further three-dimensional burnup studies both in the FEF and the LWRs, also taking into account the poisoning effects of the fission products.

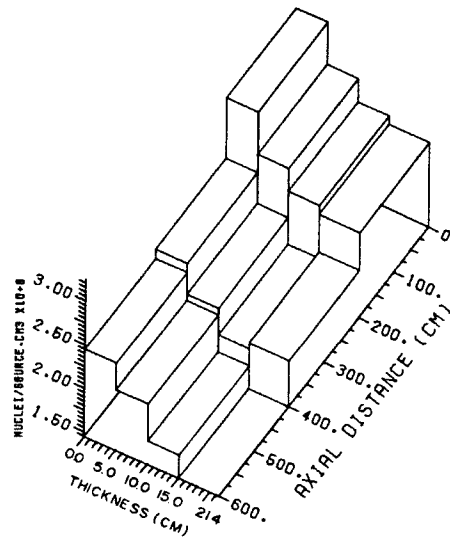
DESIGN I



FISSILE PRODUCTION DENSITY IN FUEL ASSEMBLIES VM/VF=0.0



FISSILE PRODUCTION DENSITY IN FUEL ASSEMBLIES VM/VF=0.5



FISSILE PRODUCTION DENSITY IN FUEL ASSEMBLIES VM/VF=1.0

Figure 4

DESIGN II

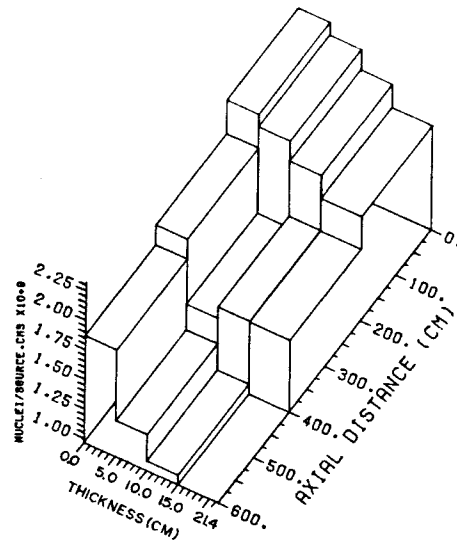
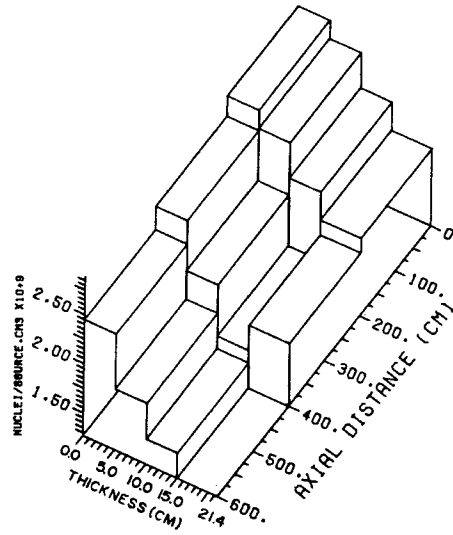
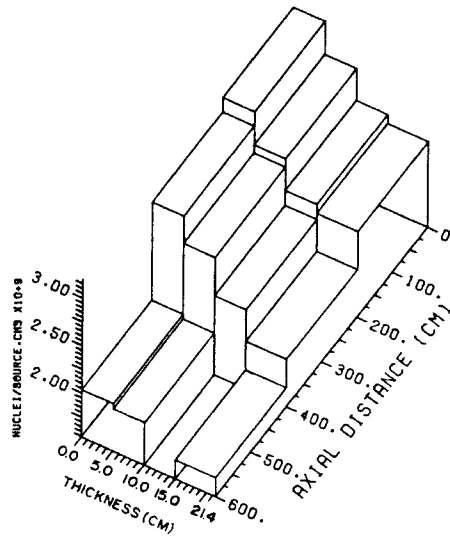
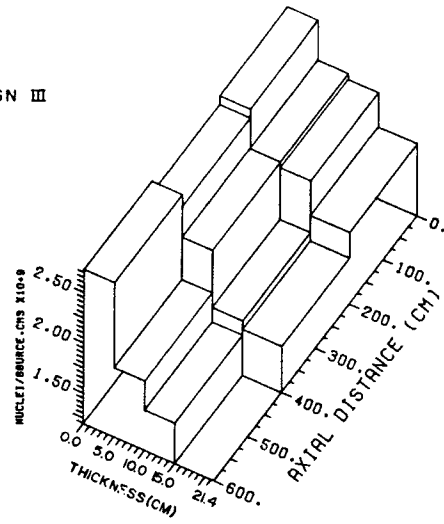
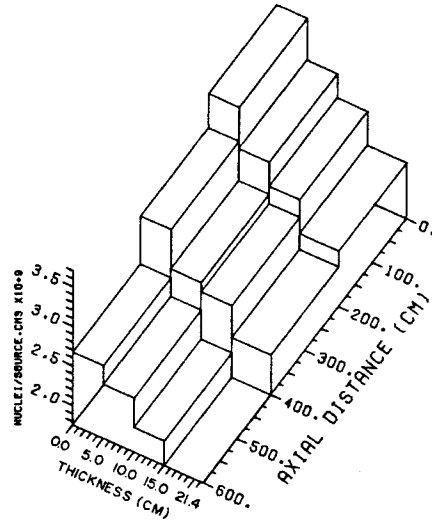
FISSILE PRODUCTION DENSITY IN FUEL ASSEMBLIES  $VM/VF=0.0$ FISSILE PRODUCTION DENSITY IN FUEL ASSEMBLIES  $VM/VF=0.6$ FISSILE PRODUCTION DENSITY IN FUEL ASSEMBLIES  $VM/VF=1.0$ 

Figure 5

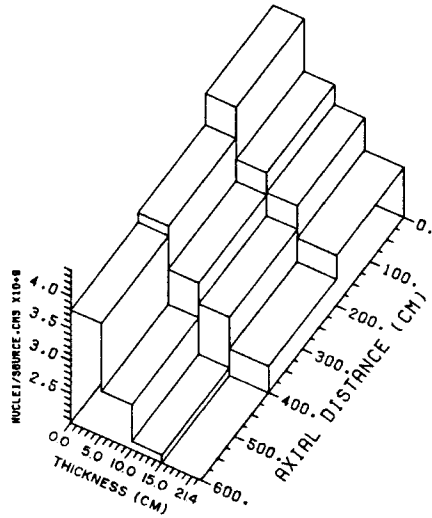
DESIGN III



FISSILE PRODUCTION DENSITY IN FUEL ASSEMBLIES VM/VF=0.0



FISSILE PRODUCTION DENSITY IN FUEL ASSEMBLIES VM/VF=0.5



FISSILE PRODUCTION DENSITY IN FUEL ASSEMBLIES VM/VF=1.0

Figure 6

In the axial direction, the peaking at the edges of the fuel subassemblies is still present. This is caused by the changing neutron spectrum as we move axially from the reactor center. This spectral effect is caused by the geometry of the reactor as a cylinder with a point source at its center, leading to different effective optical thicknesses to be seen by the neutrons as we move axially away from the center. It seems that an elaborate spectral tailoring by changing the effective optical thicknesses of the blanket regions as we move axially is needed, coupled to an irradiation and fuel management program, if an acceptable uniform irradiation is required. In some cases peaking occurs both at the reflector and plasma sides of the fuel assemblies.

Tables IX, X and XI display the fissile breeding distribution both radially and axially with the associated standard deviations for Designs I, II and III, respectively. The region numbers correspond to those in Fig. 3.

Tables XII, XIII and XIV display the tritium yield per source neutron in the radial blanket for the different designs. The contribution to tritium production from the scrapeoff zone is found to be minimal and it can be eliminated without jeopardy to the tritium breeding.

Fig. 7 shows that whereas the fissile breeding decreased as  $v_m/v_f$  increased, the fusile breeding went the opposite way, so that the two reactions are competing and one is increased or decreased at the expense of the other. Fig. 8 shows the effect of the lattice configuration in increasing the breeding densities, and consequently the time to attain a given enrichment as shown in the next section.

Table IX Th(n, $\gamma$ ) Reaction (Nuclei/Source Neutron) in Fissile Enrichment Fuel Factory in Different Radial Blanket Parts as a Function of  $v_m/v_f$ . Design I

$v_m/v_f$	Region	Central Part 0-2 m	Region	Middle Part 2-4 m	Region	Upper Part 4-6 m	Total Axially
0	5	4.99-2+3.66-3	23	4.19-2+3.25-3	41	3.87-2+2.69-3	1.31-1+5.59-3
1/2	+	3.81-2+1.99-3	+	3.66-2+2.29-3	+	3.20-2+2.46-3	1.07-1+3.91-3
1	6	3.76-2+2.43-3	24	2.96-2+2.24-3	42	2.84-2+2.45-3	9.56-2+4.11-3
0	7	4.35-2+3.56-3	25	4.02-2+3.14-3	43	2.85-2+2.22-3	1.12-1+5.24-3
1/2	+	3.71-2+2.37-3	+	3.36-2+2.35-3	+	2.50-2+1.98-3	9.57-2+3.88-3
1	8	3.23-2+2.50-3	26	2.58-2+2.04-3	44	2.50-2+2.03-3	8.31-2+3.81-3
0	9	3.95-2+3.06-3	27	3.91-2+3.39-3	45	2.57-2+2.21-3	1.04-1+5.07-3
1/2	+	3.15-2+1.88-3	+	3.12-2+2.03-3	+	2.02-2+1.68-3	8.29-2+3.24-3
1	10	2.95-2+2.39-3	28	2.25-2+2.18-3	46	2.02-2+1.75-3	7.22-2+3.68-3
0	11	4.92-2+4.46-3	29	4.90-2+4.24-3	47	3.45-2+3.01-3	1.33-1+6.85-3
1/2	+	3.98-2+3.29-3	+	3.97-2+2.69-3	+	2.76-2+2.26-3	1.07-1+4.81-3
1	12	3.65-2+2.18-3	30	3.00-2+2.92-3	48	2.20-2+1.84-3	8.85-2+4.08-3
0	Total Radially	1.82-1+7.44-3	Total Radially	1.70-1+7.06-3	Total Radially	1.27-1+5.11-3	4.79-1+1.15-2
1/2		1.47-1+4.89-3		1.41-1+4.70-3		1.05-1+4.23-3	3.93-1+7.99-3
1		1.36-1+4.76-3		1.08-1+4.74-3		9.56-2+4.07-3	3.40-1+7.85-3

Table X Th(n, $\gamma$ ) Reaction (Nuclei/Source Neutron) in Fissile Enrichment Fuel Factory in Different Radial Blanket Parts as a Function of  $v_m/v_f$ . Design II

$v_m/v_f$	Region	Central Part 0-2 m	Region	Middle Part 2-4 m	Region	Upper Part 4-6 m	Total Axially
0	5	5.39-2+4.16-3	23	4.73-2+3.75-3	41	4.34-2+2.83-3	1.45-1+6.28-3
1/2	+	4.48-2+3.22-3	+	4.16-2+2.80-3	+	3.79-2+2.43-3	1.24-1+4.92-3
1	6	3.71-2+2.38-3	24	3.54-2+2.15-3	42	2.36-2+1.66-3	9.61-2+3.61-3
0	7	5.19-2+3.86-3	25	3.48-2+2.37-3	43	2.98-2+2.35-3	1.16-1+5.10-3
1/2	+	4.22-2+2.54-3	+	3.39-2+2.28-3	+	2.94-2+2.25-3	1.06-1+4.09-3
1	8	3.34-2+2.33-3	26	3.24-2+2.03-3	44	2.32-2+1.69-3	8.90-2+3.52-3
0	9	4.81-2+3.16-3	27	3.72-2+3.43-3	45	2.47-2+2.44-3	1.10-2+5.26-3
1/2	+	3.68-2+2.30-3	+	2.59-2+1.36-3	+	2.39-2+2.13-3	8.66-2+3.42-3
1	12	2.98-2+1.52-3	28	2.80-2+2.60-3	46	1.82-2+1.55-3	7.60-2+3.39-3
0	11	5.63-2+5.30-3	29	4.79-2+4.84-3	47	2.94-2+3.06-3	1.33-1+7.80-3
1/2	+	4.18-2+2.36-3	+	3.87-2+2.84-3	+	2.57-2+1.78-3	1.06-1+4.10-3
1	12	3.70-2+2.12-3	30	3.10-2+2.55-3	48	2.65-2+2.30-3	9.45-2+4.04-3
0	Total Radially	2.10-1+8.38-3	Total Radially	1.67-1+7.41-3	Total Radially	1.27-1+5.37-3	5.04-1+1.24-2
1/2		1.66-1+5.26-3		1.40-1+4.79-3		1.17-1+4.32-3	4.23-1+8.32-3
1		1.37-1+4.23-3		1.27-1+4.69-3		9.15-2+3.65-3	3.56-1+7.29-3

Table XI Th(n, $\gamma$ ) Reaction (Nuclei/Source Neutron) in Fissile Enrichment Fuel Factory in Different Radial Blanket Parts as a Function of  $v_m/v_f$ . Design III

$v_m/v_f$	Region	Central Part 0-2 m	Region	Middle Part 2-4 m	Region	Upper Part 4-6 m	Total Axially
0 1/2 1	5 + 6	6.25-2+4.01-3 5.74-2+3.13-3 5.11-2+2.64-3	23 + 24	6.05-2+4.54-3 5.08-2+2.70-3 4.56-2+3.07-3	41 + 42	6.33-2+4.83-3 4.14-2+2.34-3 4.39-2+2.94-3	1.86-1+7.75-3 1.50-1+4.75-3 1.41-2+5.00-3
0 1/2 1	7 + 8	5.39-2+4.90-3 4.97-2+2.59-3 4.22-2+2.51-3	25 + 26	5.39-2+4.76-3 4.34-2+3.13-3 3.83-2+2.00-3	43 + 44	4.41-2+3.75-3 3.80-2+2.44-3 3.20-2+1.86-3	1.52-1+7.79-3 1.31-1+4.74-3 1.13-1+3.71-3
0 1/2 1	9 + 10	5.28-2+4.24-3 4.53-2+3.00-3 3.90-2+2.43-3	27 + 28	4.08-2+3.51-3 4.18-2+1.87-3 3.48-2+2.06-3	45 + 46	3.75-2+3.23-3 3.24-2+2.21-3 2.56-2+2.00-3	1.31-1+6.38-3 1.20-1+4.17-3 9.94-2+3.76-3
0 1/2 1	11 + 12	5.80-2+6.22-3 4.99-2+2.84-3 4.28-2+2.68-3	29 + 30	5.02-2+4.99-3 4.58-2+2.98-3 3.73-2+2.67-3	47 + 48	3.63-2+3.19-3 3.56-2+2.71-3 3.11-2+2.53-3	1.45-1+8.59-3 1.31-1+4.93-3 1.11-1+4.55-3
0 1/2 1	Total Radially	2.27-1+9.84-3 2.02-1+5.79-3 1.75-1+5.13-3	Total Radially	2.05-1+8.97-3 1.82-1+5.43-3 1.56-1+4.98-3	Total Radially	1.81-1+7.62-3 1.47-1+4.86-3 1.33-1+4.74-3	6.13-1+1.53-2 5.31-1+9.31-3 4.64-1+8.58-3



Table XII Tritium Breeding in Different Parts of Radial Blanket (Nuclei/Source Neutron) of Fissile Enrichment Fuel Factory as a Function of  $v_m/v_f$   
Design I

$v_m/v_f$	Region	Central Part 0-2 m		Region	Middle Part 2-4 m		Region	Upper Part 4-6 m		Total Axially	
		T6	T7		T6	T7		T6	T7	T6	T7
0	3	1.80-2+1.70-3	5.31-3+9.49-4	21	1.45-2+1.09-3	3.97-3+9.12-4	39	1.22-2+1.12-3	2.92-3+6.24-4	4.47-2+2.31-3	1.22-2+1.46-3
1/2		1.77-2+9.40-4	3.90-3+7.26-4		1.79-2+1.13-3	4.17-3+6.77-4		1.50-2+1.55-3	1.51-3+3.39-4	5.06-2+2.14-3	9.58-3+1.05-3
1		2.29-2+1.71-3	4.58-3+7.19-4		2.06-2+1.91-3	4.09-3+1.35-3		1.68-2+1.41-3	2.32-3+6.60-4	6.03-2+2.93-3	1.10-2+1.67-3
0	17	8.83-2+4.72-3	4.02-3+1.11-3	35	8.79-2+6.84-3	3.40-3+8.27-4	53	5.70-2+4.84-3	4.75-3+1.69-3	2.33-1+9.62-3	1.22-2+2.18-3
1/2		1.09-1+6.44-3	3.66-3+1.02-3		1.10-1+8.87-3	3.62-3+1.15-3		6.18-2+5.35-3	1.07-3+4.17-4	2.81-1+1.22-2	8.35-3+1.59-3
1		1.32-1+9.84-3	4.56-3+1.01-3		1.14-1+8.83-3	1.62-3+6.19-4		6.64-2+5.54-3	3.08-3+1.41-3	3.12-1+1.43-2	9.26-3+1.84-3
0	19	1.49-2+2.93-3	-	37	1.66-2+3.88-3	-	55	1.07-2+2.30-3	1.39-5+1.39-5	4.22-2+5.38-3	1.39-5+1.39-5
1/2		1.82-2+4.16-3	-		1.76-2+3.83-3	-		1.21-2+2.59-3	-	4.79-2+6.22-3	-
1		2.32-2+5.30-3	9.22-5+9.22-5		1.88-2+2.88-3	-		7.30-3+1.70-3	-	4.93-2+6.27-3	9.22-5+9.22-5
0	Total Radially	1.21-1+5.81-3	9.33-3+1.46-3	Total Radially	1.19-1+7.94-3	7.37-3+1.23-3	Total Radially	7.99-2+5.47-3	7.68-3+1.80-3	3.20-1+1.13-2	2.44-2+2.62-3
1/2		1.45-1+7.72-3	7.56-3+1.25-3		1.46-1+9.73-3	7.79-3+1.33-3		8.99-2+6.14-3	2.58-3+5.37-4	3.80-1+1.39-2	1.79-2+1.89-3
1		1.78-1+1.13-2	9.23-3+1.24-3		1.53-1+9.48-3	5.71-3+1.49-3		9.05-2+5.96-3	5.40-3+1.56-3	4.22-1+1.58-2	2.04-2+2.49-3

T6 and T7 are tritium yields from reactions with  $^6\text{Li}$  and  $^7\text{Li}$

Table XIII

Tritium Breeding in Different Parts of Radial Blanket (Nuclei/Source Neutron) of Fissile Enrichment Fuel Factory as a Function of  $v_m/v_f$ .  
Design II

$v_m/v_f$	Region	0-2m Height		Region	2-4m Height		Region	4-6m Height		Total Axially	
		T6	T7		T6	T7		T6	T7	T6	T7
0	3	1.96-2+1.21-3	3.16-3+6.85-4	21	1.77-2+1.26-3	5.26-3+1.01-3	39	1.27-2+1.36-3	2.78-3+6.39-4	5.00-2+2.21-3	1.12-2+1.38-3
1/2		2.37-2+1.92-3	3.22-3+7.37-4		1.95-2+1.29-3	2.99-3+6.60-4		2.02-2+1.54-3	2.07-3+5.82-4	6.34-2+2.78-3	8.28-3+1.15-3
1		2.61-2+1.65-3	4.43-3+9.88-4		2.69-2+1.98-3	2.85-3+7.49-4		1.58-2+1.13-3	4.17-3+1.35-4	6.88-2+2.81-3	1.15-2+1.25-3
0	15	1.55-2+1.96-3	9.85-4+4.07-4	33	1.30-2+1.61-3	7.73-4+3.98-4	51	7.04-3+9.67-4	7.25-4+3.65-4	3.55-2+2.71-3	2.48-3+6.76-4
1/2		1.62-2+1.19-3	1.02-3+3.98-4		1.42-2+1.25-3	2.68-4+1.80-4		8.69-3+1.11-3	1.61-4+1.61-4	3.91-2+2.05-3	1.45-3+4.66-4
1		1.48-2+1.20-3	3.07-4+1.67-4		1.49-2+1.89-3	8.09-4+4.17-4		1.21-2+1.09-3	1.41-4+1.39-4	4.18-2+2.49-3	1.26-3+4.70-4
0	17	8.39-2+7.02-3	1.40-3+8.81-4	35	7.59-2+4.94-3	3.34-3+9.65-4	53	4.58-2+6.74-3	1.19-3+7.66-4	2.06-1+1.09-2	5.93-3+1.51-3
1/2		8.48-2+6.95-3	7.79-4+3.60-4		7.28-2+5.01-3	2.74-4+2.74-4		5.50-2+5.53-3	3.21-4+2.22-4	2.13-1+1.02-2	1.37-3+5.04-4
1		9.83-2+6.79-3	1.76-3+6.85-4		8.69-2+8.69-3	1.00-3+6.49-4		6.52-2+5.49-3	4.83-4+4.83-4	2.50-1+1.23-2	3.24-3+1.06-3
0	19	9.90-3+2.50-3	-	37	1.18-2+3.32-3	-	55	4.50-3+1.63-3	-	2.62-2+4.46-3	-
1/2		1.25-2+3.72-3	-		9.62-3+2.51-3	-		6.93-3+1.82-3	-	2.91-2+4.84-3	-
1		1.15-2+2.40-3	-		1.16-2+2.75-3	-		6.22-3+1.66-3	-	2.93-2+4.01-3	-
0	Total Radially	1.29-1+7.80-3	5.55-3+1.19-3	Total Radially	1.18-1+6.29-3	9.37-3+1.45-3	Total Radially	7.00-2+7.13-3	4.70-3+1.06-3	3.18-1+1.23-2	1.96-2+2.15-3
1/2		1.37-1+8.20-3	5.02-3+9.12-4		1.16-1+5.88-3	3.53-3+7.37-4		9.08-2+6.12-3	2.55-3+6.43-4	3.45-1+1.18-2	1.11-2+1.34-3
1		1.51-1+7.49-3	6.50-3+1.21-3		1.40-1+9.52-3	4.66-3+1.08-3		9.93-2+5.95-3	4.79-3+5.20-4	3.90-1+1.35-2	1.60-2+1.70-3

T6 and T7 are tritium yields from reactions with  ${}^6\text{Li}$  and  ${}^7\text{Li}$

Table XIV

Tritium Breeding in Different Parts of Radial Blanket (Nuclei/Source Neutron) of Fissile Enrichment Fuel Factory as a Function of  $v_m/v_f$ .  
Design III

$v_m/v_f$	Region	0-2m Height		Region	2-4m Height		Region	4-6m Height		Total Axially	
		T6	T7		T6	T7		T6	T7	T6	T7
0	3	2.37-2+1.74-3	2.90-3+5.50-4	21	2.21-2+1.43-3	2.87-3+8.54-4	39	1.86-2+1.20-3	1.49-3+5.81-4	6.44-2+2.55-3	7.26-3+1.17-3
1/2		3.18-2+1.73-3	5.55-3+1.27-3		2.73-2+2.11-3	2.96-3+8.28-4		2.36-2+1.76-3	1.52-3+4.57-4	8.27-2+3.25-3	1.00-2+1.58-3
1		3.85-2+3.11-3	3.57-3+7.96-4		2.97-2+2.34-3	3.58-3+8.66-4		3.52-2+2.67-3	1.40-3+4.16-4	1.03-1+4.72-3	8.55-3+1.25-3
0	15	1.33-2+1.32-3	1.54-3+5.45-4	33	1.37-2+1.64-3	9.37-4+5.55-4	51	8.85-3+1.33-3	1.84-4+1.84-4	3.59-2+2.49-3	2.66-3+7.99-4
1/2		1.75-2+1.87-3	7.50-4+3.03-4		1.63-2+1.21-3	8.39-4+3.97-4		1.27-2+1.57-3	2.77-4+1.60-4	4.65-2+2.73-3	1.87-3+5.24-4
1		2.22-2+2.20-3	2.53-4+1.73-4		2.00-2+1.41-3	7.52-4+3.98-4		1.51-2+1.93-3	1.86-7+1.86-7	5.73-2+3.25-3	9.25-4+4.34-4
0	17	7.34-2+6.71-3	1.09-3+4.37-4	35	7.05-2+7.00-3	4.89-4+2.67-4	53	5.22-2+5.35-3	1.67-4+1.12-4	1.96-1+1.11-2	1.75-3+5.24-4
1/2		9.42-2+8.41-3	2.03-3+7.21-4		8.93-2+5.72-3	9.88-4+6.94-4		6.32-2+6.20-3	9.70-4+7.05-4	2.47-1+1.19-2	3.99-3+1.22-3
1		1.16-1+1.04-2	2.74-3+1.06-3		9.26-2+8.18-3	7.32-4+4.08-4		7.10-2+3.53-3	2.01-4+2.01-4	2.80-1+1.37-2	3.67-3+1.15-3
0	19	1.41-2+2.59-3	-	37	8.96-3+2.57-3	-	55	9.50-3+3.22-3	-	3.26-2+4.87-3	-
1/2		1.46-2+2.79-3	-		1.29-2+2.77-3	-		6.35-3+1.57-3	-	3.39-2+4.23-3	-
1		1.84-2+2.93-3	-		1.19-2+1.95-3	2.03-4+2.03-4		1.06-2+2.60-3	-	4.09-2+4.38-3	2.03-4+2.03-4
0	Total Radially	1.25-1+7.52-3	5.53-3+8.89-4	Total Radially	1.15-1+7.77-3	4.30-3+1.05-3	Total Radially	8.92-2+6.50-3	1.84-3+5.20-4	3.29-1+1.26-2	1.17-2+1.51-3
1/2		1.58-1+9.22-3	8.33-3+1.49-3		1.46-1+6.80-3	4.79-3+1.15-3		1.06-1+6.82-3	2.77-3+3.55-4	4.10-1+1.33-2	1.59-2+2.07-3
1		1.95-1+1.15-2	6.56-3+1.34-3		1.54-1+8.84-3	5.27-3+1.06-3		1.32-1+8.48-3	1.60-3+4.62-4	4.81-1+1.55-2	1.34-2+1.77-3

T6 and T7 are tritium yields from reactions with  $^6\text{Li}$  and  $^7\text{Li}$

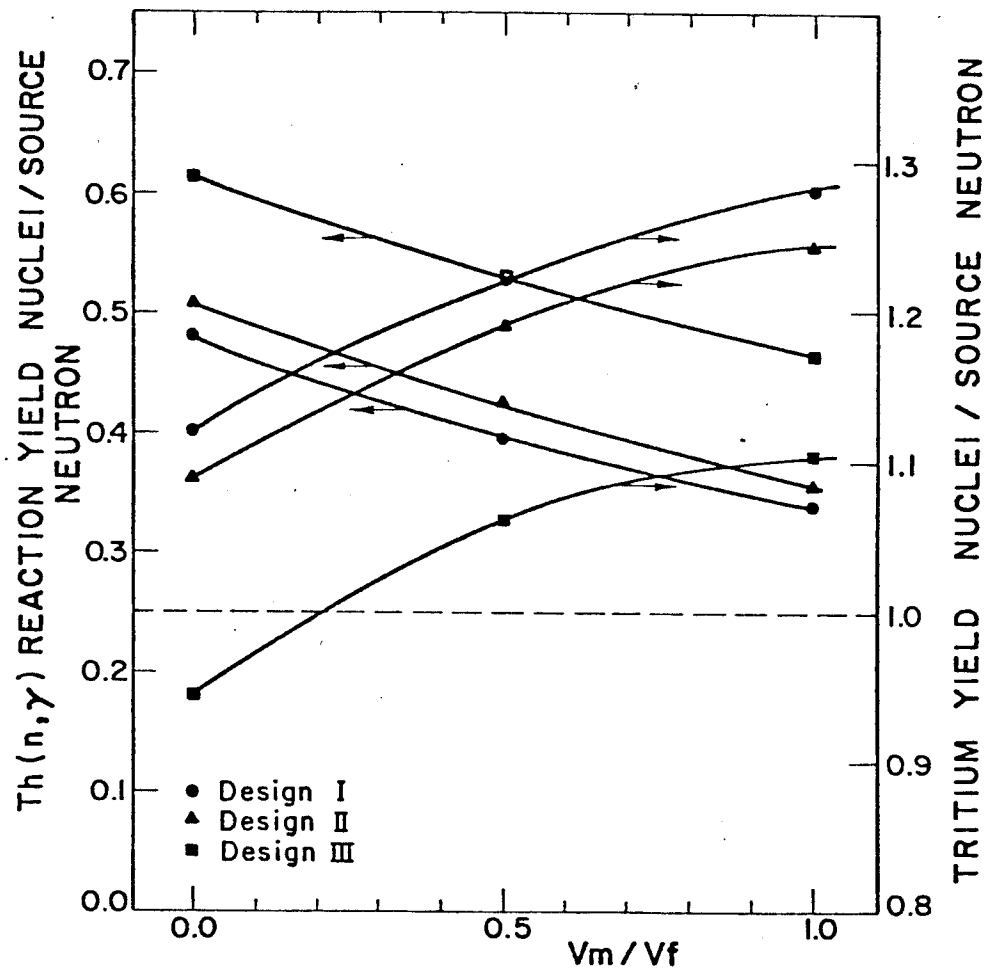


Figure 7

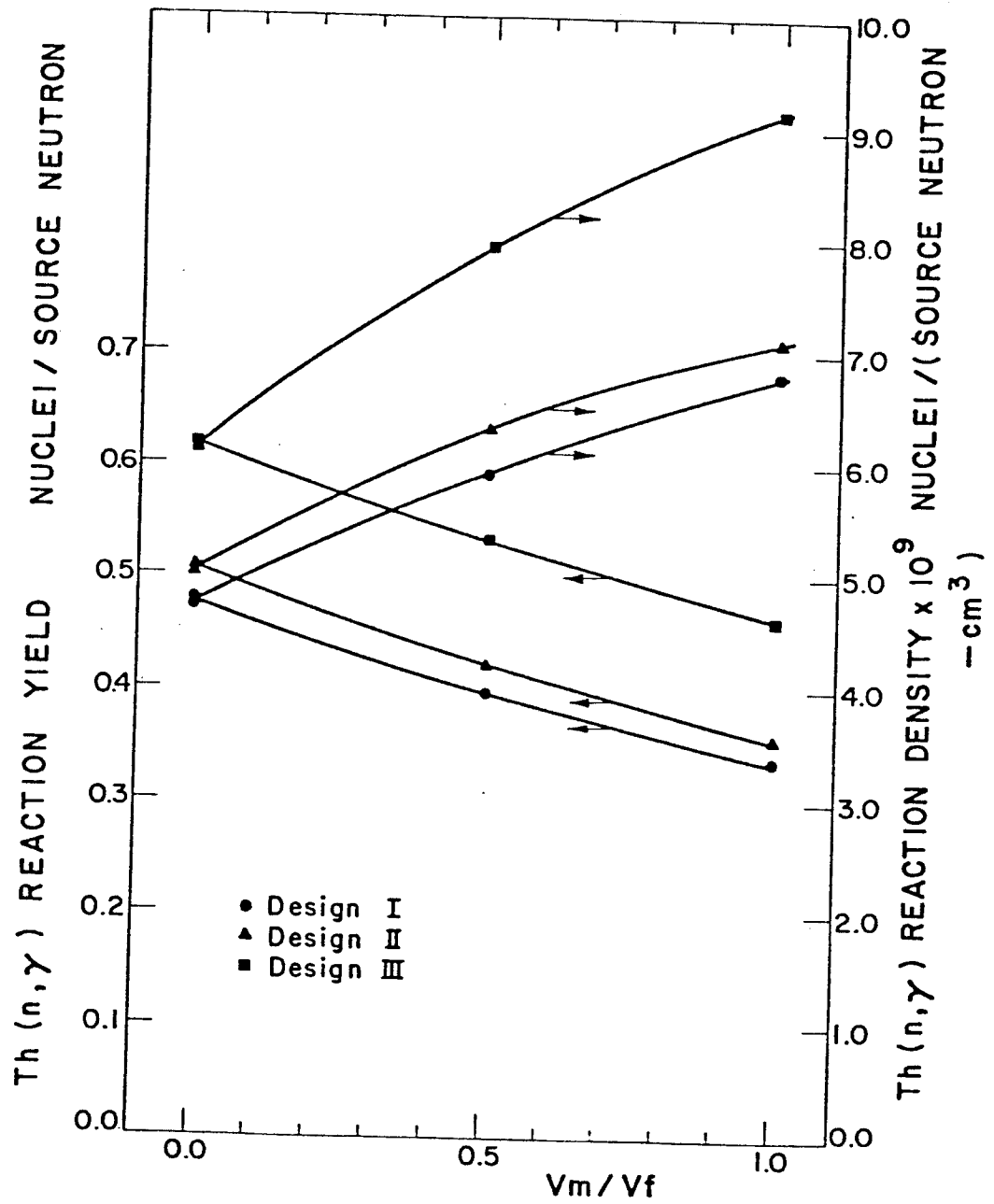


Figure 8

### 3.3 Economic Considerations

In Table XV we show the yearly fissile production for Designs I, II and III for different values of  $v_m/v_f$ .

The fissile fuel production per year has been calculated from the relationship:

$$K\left(\frac{v_m}{v_f}\right) = U\left(\frac{v_m}{v_f}\right) \cdot S_n \cdot \frac{M_f}{A_v} \cdot Y \left(\frac{g}{year}\right) \quad (1)$$

where:  $U\left(\frac{v_m}{v_f}\right)$  is the fissile nuclei yield per source neutron,

$S_n$  is the 14.06 MeV neutron source ( $4.005 \times 10^{20} \frac{\text{neutrons}}{\text{sec}}$ ),

$\frac{v_m}{v_f}$  is the neutron multiplier-moderator to fuel volume ratio,

$Y = 3.154 \times 10^7$  is a conversion ratio from year to seconds.

It can be noticed from the results of Table XV that a reduction in the fuel inventory by going from  $\frac{v_m}{v_f} = 0$  to 0.5 and 1.0, corresponds to slower reduction in the yearly fissile fuel production. This is caused by the higher breeding densities achieved by the suggested lattice configuration. This will also lead to a reduction in the time required to attain a certain fuel enrichment, as shown below.

Let us first define the "enrichment potential:  $r$ " as:

$$r = \frac{\text{Total weight of fissile fuel material}}{\text{Initial inventory of fertile material}} \cdot$$

Table XV Economic Parameters for Fissile Enrichment Fuel  
Factory as a Function of  $v_m/v_f$  for Designs I, II and III

Design	$v_m/v_f$	Yearly Production <sup>233</sup> U) of Fissile Fuel (MT /year)	Time to attain an Average 3% En- richment in Fresh Fuel Batch (years)	Present Value of Future Yearly Income on the Sale of Fissile Fuel (106 \$/year)			Reduction in Fuel Inventory (Percentage)
				Discount Rate			
				10%	15%	20%	
I	0.0	2.33	3.46	83.8	71.8	62.0	0
	0.5	1.92	2.80	73.5	64.9	57.6	33
	1.0	1.66	2.43	65.8	59.1	53.3	50
II	0.0	2.45	3.29	89.5	77.3	67.2	0
	0.5	2.07	2.59	80.9	72.1	64.5	33
	1.0	1.74	2.31	69.8	63.0	57.1	50
III	0.0	2.98	2.70	115.2	102.2	91.1	0
	0.5	2.60	2.06	106.8	97.5	89.3	33
	1.0	2.27	1.77	95.9	88.6	82.2	50

Assumed Fissile Fuel Price: \$50/g  $^{233}\text{U}$ .  
Th(n, $\gamma$ ) reaction is considered as the  $^{233}\text{U}$  producing reaction. No burnup was considered.

Notice that the "enrichment" is usually defined as:

$$r' = \frac{\text{Weight of Fissile Material}}{\text{Total Fuel Weight (Fertile \& Fissile)}} .$$

Now the time in years to attain a potential enrichment  $r$  can be expressed as:

$$\tau_r \left( \frac{v_m}{v_f} \right) = \frac{r}{\frac{K \left( \frac{v_m}{v_f} \right)}{v_{fr}}} \left\{ v_{fr} \left( \frac{v_m}{v_f} \right) \alpha_{fm} \rho(fm) \cdot \left( \frac{\rho(f)}{\rho(fm)} \right) \right\} (\text{years}) \quad (2)$$

where  $r$  is the already defined enrichment potential,

$\frac{v_m}{v_f}$  is the neutron multiplier/moderator to fuel volume ratio,

$v_{fr}$  is the volume of the fuel region ( $\text{cm}^3$ ),

$K$  is the yearly production of fissile fuel ( $\frac{\text{g}}{\text{year}}$ ),

$\alpha_{fm}$  is the volume fraction of fuel material ( $\text{ThO}_2$ ) in the fuel plus coolant region (30.3695% in our design),

$\rho(fm)$  is the density of fuel material,  $\rho(\text{ThO}_2) = 10.01 \frac{\text{g}}{\text{cm}^3}$ ,

$\frac{\rho(f)}{\rho(fm)}$  is the weight fraction of fuel in fuel material; for  $\text{ThO}_2$ :

$$\frac{\rho(\text{Th})}{\rho(\text{ThO}_2)} = 0.8788.$$

As shown in Table XV,  $\tau_r$  can be substantially reduced, particularly for Design III, by using the suggested lattice configuration and a neutron multiplier zone in front of the axial blanket, at the expense of a reduction



in the overall fissile fuel production, and a substantial reduction in the fuel inventory. Reduction of the fuel inventory will decrease the capital cost of the installation. Shorter enrichment times lead to longer possible residence times in the LWRs.

A simple formula for the present value of the future yearly income on the sale of the fissile fuel can be written as:

$$W\left(\frac{v_m}{v_f}\right) = \frac{K\left(\frac{v_m}{v_f}\right) \cdot L}{(1+i)^{\tau_r} \left(\frac{v_m}{v_f}\right)} \quad (\$/\text{year}) \quad (3)$$

where  $i$  is a discount rate (e.g. 15%)

$\tau_r$  and  $K$  are as defined in Eqns. 1 and 2, respectively,

$L$  is the sale price of the fissile fuel (\$/gm).

To choose a representative value of  $L$  we use the economic analysis of Cook and Lidsky<sup>(4)</sup> for a molten-salt fusion hybrid. In one scenario they hypothesized that the reactor economy would continue to be dominated by LWRs, that Pu recycle would not occur, but that the required separative work capacity would be built as a result of tremendous demand. In this case they estimate that U-233 would be worth \$33-\$48/gm, and the demand for fissile fuel would be  $1.2-3.5 \times 10^2$  tonnes/year. In a second scenario they assume that Liquid Metal Fast Breeders (LMFBRs) will not enter the market but high conversion reactors do. In this case the U-233 worth is \$80-\$100/gm and the demand is expected to stabilize around  $0.3-0.9 \times 10^2$  tonnes/year in 2000 A.D. Taking a value of  $L = \$50/\text{gm}$ , the present value of yearly income on the sale of fissile fuel from Eqn. 3 is shown to decrease slower for Design III as a function

of  $v_m/v_f$  than Designs I and II. Thus, the shortened time to attain a given enrichment keeps the yearly income from the sale of the fissile fuel from decreasing fast, even though its yearly production is lowered. Obviously, we have the added advantage of a reduced fuel inventory. A more detailed economic analysis will be reported in the future,

It can be noticed that Design III is superior to Design I both in overall yearly fissile production and the time required to attain a given enrichment. If Design I for  $v_m/v_f = 0.0$  is considered as a base case arrived at from one-dimensional scoping studies, then Design III for  $v_m/v_f = 1.0$  from three-dimensional studies leads to almost the same fissile fuel production with about half the time to attain a given enrichment, together with a 50% reduction in the fuel inventory.

#### 4. Conclusions and Recommendations

Our study suggests that the adoption of the suggested lattice configuration achieves its intended purpose of increasing the breeding densities in the fertile fuel, leading in turn to shorter times in the FEFF to attain a given average enrichment. This is also associated with a reduction in the fuel inventory with corresponding economic and safety implications. However, this is accomplished at the expense of a reduction in the overall fissile fuel production. Materials other than Pb with low parasitic absorption need be investigated as lattice scatterer materials. Preceding the tritium-breeding axial blanket by a Pb multiplying zone is found to increase the fissile breeding in the radial blanket at the expense of a reduction of tritium breeding in the axial blanket, and is recommended as a design feature.

The neutronic coupling between the axial and radial blankets questions the validity of simple solid angle weighting of one-dimensional calculations used in some previous studies. Severe nonuniformities in the spatial distribution of the fissile enrichment are detected radially and axially. The design of detailed spectra shaping and on-line fuel irradiation and management programs is necessary for the eventual application of such a concept. Detailed burnup and economic calculations for both the FEF and the LWRs are needed to assess the FEF's commercial feasibility. Further neutronics cell calculations considering the fuel pins in the fuel assemblies and self-shielded cross-section data are needed for more reliable estimates of breeding. Irradiation of single fuel pins rather than whole fuel assemblies would offer an alternative concept alleviating nonuniformity problems. Enrichment of single fuel pellets embedded in graphite spheres, in a pebble bed concept, then assembling them into fuel pins and assemblies, would provide uniform enrichment, and is an interesting concept which needs investigation.

## Appendix

### One-Dimensional Discrete Ordinates and Monte Carlo Scoping Studies

Scoping one-dimensional calculations preceded the three-dimensional calculations. To check the Monte Carlo modelling and modifications to the used Monte Carlo code used in this study, a one-dimensional spherical model of the treated blanket, as shown in Fig. A-1, was analyzed by both Monte Carlo and discrete ordinates using the ANISN code.<sup>(32)</sup> A comparison of the results is shown in Table A-1. In the same table, it is shown that replacing the Li zone by Pb as a neutron multiplier increases the  $\text{Th}(n,\gamma)$  reaction substantially which suggested including a Pb zone before the reflector in Designs II and III. These have in fact a higher fissile production in the three-dimensional analysis than Design I. The latter corresponds to the one-dimensional model, except for the reactor radius which was changed from 5 to 6 m for radiation damage to the first wall requirements. In case the Li zones are replaced by Pb in Table A-1, no tritium is produced and the FEFF becomes a fissile producer. Replacing the Li by a vacuum does not lead to as high a fissile production because of the increased neutron leakage. If only the axial blanket in the FEFF is used for tritium production, the design of the radial blanket may be simplified, but additional tritium breeding would have to be achieved in the LWRs themselves, complicating in turn their design.

If one would use solid angle weighting for results from one-dimensional studies; for a solid angle of 0.707, the  $\text{Th}(n,\gamma)$  production per source neutron in the radial blanket would be estimated as:  $0.934 \times 0.707 = 0.660$ . However, 3-D studies for the same system give a value of 0.479. The tritium breeding in the radial blanket would be estimated as:  $0.624 \times 0.707 = 0.441$ . For a breeding ratio of 1.5 the axial blanket would contribute:  $1.5 \times 0.293 = 0.440$ , giving a total 0.881 triton/source neutron.

# MATERIALS COMPOSITIONS

1000	Inner Vacuum
1	82.2 v/o Pb + 9.3 v/o Na + 8.5 v/o Zircalloy-2
2	95 v/o Nat. Lithium + 5 v/o Stainless Steel
3	Stainless Steel
4	30.3 v/o ThO + 9.2 v/o Zircalloy-2 + 1.3 v/o Void + 59.2 v/o Na Coolant
5	33 v/o Pb + 67 v/o C
0	Outer Vacuum

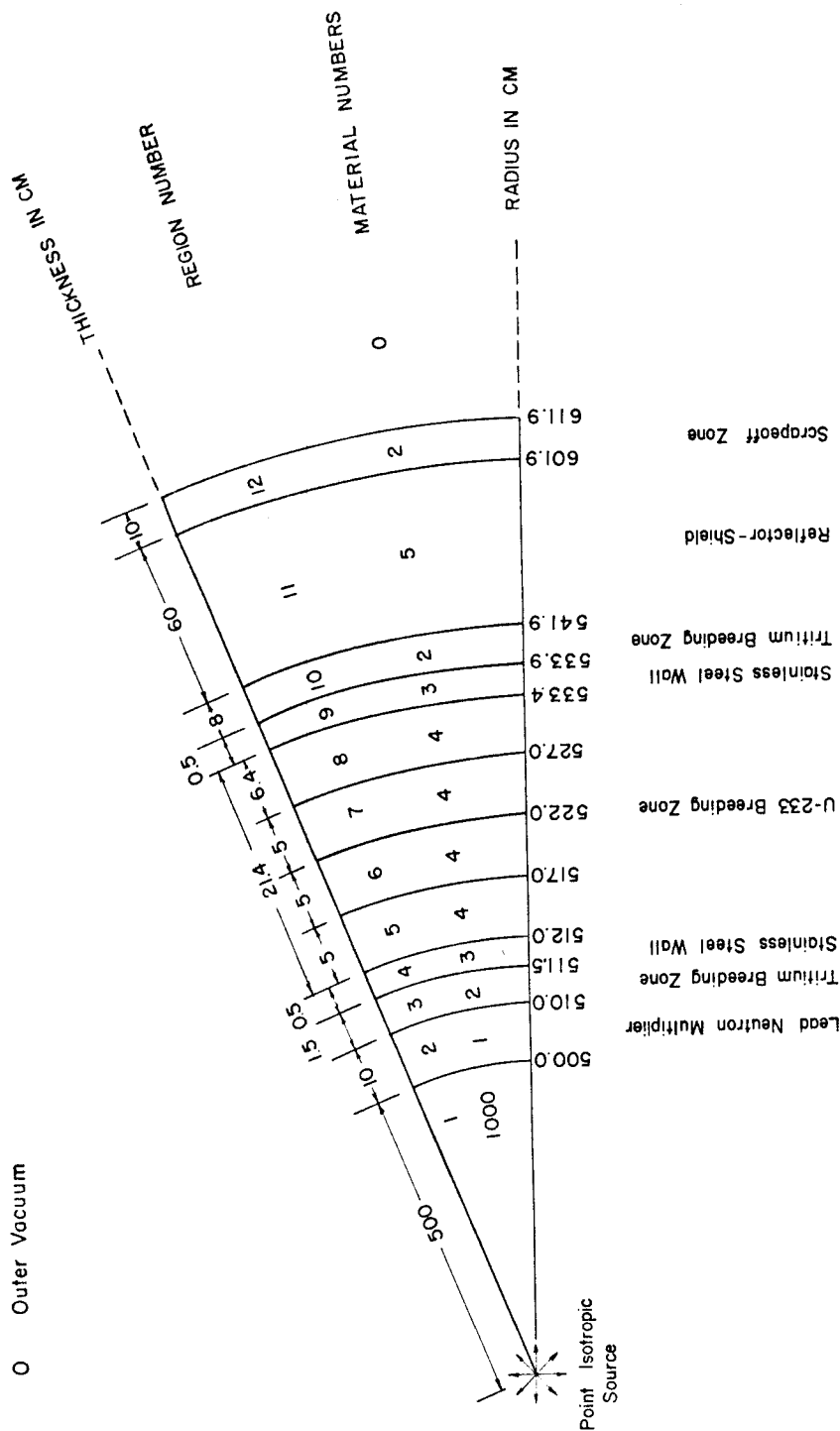


Figure A-1

The 3-D study again disagrees and gives a value of 1.112 for this case. The sum of the  $\text{Th}(n,\gamma)$  reaction and the number of tritons produced per source neutron are, however, 1.541 for the 1-D solid angle-weighted estimate, and 1.591 from the 3-D study, so that 1-D solid angle-weighted estimates would fail to adequately apportion the  $\text{Th}(n,\gamma)$  and tritium production in such a system, even though useful for preliminary studies.

Table A.1 Comparison of Different One-Dimensional Blanket Compositions and Configurations With Respect to Breeding

Reaction	Region						Total
	3	5	6	7	8	10	12
$\text{Th}(n,\gamma)\text{U}$	-	2.83-1 <sup>+</sup> 2.80-1+1.35-2* 3.64-1+1.20-2** 3.06-1+9.98-3***	2.28-1 2.28-1+1.06-2 2.76-1+6.78-3 2.51-1+1.01-2	1.95-1 2.01-1+5.38-3 2.55-1+1.04-2 2.26-1+7.65-3	2.28-1 2.26-1+8.39-3 4.03-1+1.40-2 4.47-1+1.93-2	-	9.34-1 9.35-1+1.98-2 1.30+0+2.22-2 1.23+0+2.52-2
${}^6\text{Li}(n,\alpha)\text{T}$	1.04-1 1.05-1+7.42-3 0.0 0.0	-	-	-	-	4.16-1 3.89-1+2.01-2 0.0 0.0	7.67-2 7.76-2+1.09-2 0.0 0.0
${}^7\text{Li}(n,n'\alpha)\text{T}$	1.30-2 1.55-2+7.42-3 0.0 0.0	-	-	-	-	1.40-2 1.69-2+2.70-3 0.0 0.0	7.47-5 1.82-4+1.82-4 0.0 0.0
Total Tritium	1.17-1 1.21-1+8.04-3 0.0 0.0	-	-	-	-	4.30-1 4.06-1+2.03-2 0.0 0.0	7.68-2 7.78-2+1.09-2 0.0 0.0

+ Discrete ordinates P3-S4.  
 \* Regions 3, 10 and 12 are: 95 v/o natural lithium + 5 v/o stainless steel. Leakage = 1.03-2.  
 \*\* Regions 3, 10 and 12 are: 82.2 v/o Pb + 9.3 v/o Na + 8.5 v/o Zircaloy-2. Leakage = 8.27-2.  
 \*\*\* Regions 3, 10 and 12 are: Vacuum. Leakage = 1.42-1.  
 All were 800 histories, 20 experiments cases.

### References

1. R.W. Conn, et al., "SOLASE-H, A Laser Fusion Hybrid Study", UWFD-270, Fusion Research Program, The University of Wisconsin (Oct. 1978).
2. H.A. Bethe, "The Fusion Hybrid", Nuclear News, pp. 41-44 (May 1978).
3. R.W. Conn, S.I. Abdel-Khalik, G. Moses, and M. Youssef, "The SOLASE-H Laser Fusion Hybrid", Trans. Am. Nucl. Soc., 30 (1978), p. 58.
4. A.G. Cook and L.M. Lidsky, "The Feasibility of U-233 Breeding in Deuterium-Tritium Fusion Devices", MIT Report (March 1977).
5. M.M.H. Ragheb and T.H. Higgins, Book Review: "P. Silvennoimen, Reactor Core Fuel Management", IEEE Transactions on Nuclear Science, Vol. NS-25, N.3 (1978).
6. M.M.H. Ragheb and T.H. Higgins, Book Review: "J.O. McVeigh, Sun Power: An Introduction to the Applications of Solar Energy", IEEE Transactions on Nuclear Science, Vol. NS-25, N.3 (1978).
7. C.W. Gordon and A.A. Harms, "The Basic Characteristics of an Efficient Fusion Breeder", Atomkernenergie (ATKE) Bd. 29, Lfg. 3, p. 213 (1977).
8. L.M. Lidsky, "Fission-Fusion Systems: Hybrid, Symbiotic and Auger", Nucl. Fusion 15, p. 151 (1975).
9. G. Lavergne, J.E. Robinson and J.G. Martel, "On the Matching of Fusion Breeders to Heavy Water Reactors", Nucl. Tech. 26, p. 12 (1975).
10. D.J. Bender, "Performance Parameters for Fusion-Fission Power Systems", UCRL-80589, Rev. 1, Lawrence Livermore Laboratory (May 1978).
11. J. Maniscalco, "Fusion-Fission Hybrid Concepts for Laser-Induced Fusion", Nuclear Technology, Vol. 28, pp. 98-107 (January 1976).
12. A.G. Cook and J.A. Maniscalco, "Uranium 233 Breeding and Neutron Multiplying Blankets for Fission Reactors", Nuclear Technology, Vol. 30 (July 1976).
13. D.T. Aase, et al., "TCT Hybrid Preconceptual Blanket Design Studies", PNL-2304, UC-20, Battelle Pacific Northwest Laboratories (January 1978).
14. S.S. Rozhkov and G.E. Shatalov, "Thorium in the Blanket of a Hybrid Thermonuclear Reactor", US-USSR Symposium on Fusion-Fission Reactors, July 13-16, 1976, Livermore, California, CONF-760733, p. 143 (1976).



15. V.V. Kotov, C.W. Maynard, D.V. Makovskiy and G.E. Shatalov, "Sensitivity Analysis of Parameters of Hybrid Reactor to Nuclear Data", Kurchatov Institute Report IAE-2817 (1977).
16. R.W. Conn, G.A. Moses, and S.I. Abdel-Khalik, "Notes on Fusion Hybrid Reactors", UWFDM-240, Fusion Research Program, The University of Wisconsin (April 1978).
17. M.M.H. Ragheb, M.Z. Youssef, S.I. Abdel-Khalik and C.W. Maynard, "Three-Dimensional Lattice Calculations for a Laser-Fusion Fissile-Enrichment Fuel Factory", Trans. Am. Nucl. Soc. 30 (1978), p. 59. See also UWFDM 263,264.
18. H.A. Feiveson, T.B. Taylor, F. von Hippel, and R.H. Williams, "The Plutonium Economy: Why We Should Wait and Why We Can Wait", Bulletin of the Atomic Scientists, p. 10 (December 1976).
19. C.M. Lederer, J.M. Hollander, and I. Perlman, "Table of Isotopes", Sixth Edition, John Wiley and Son, Inc. (1968).
20. D.C. Kocher, "Nuclear Decay Data for Radionuclides Occurring in Routine Releases From Nuclear Fuel Cycle Facilities", ORNL/NUREG/TM-102 (August 1977).
21. M.M. Ragheb, E.T. Cheng, and R.W. Conn, "Monte Carlo Study of Asymmetric Effects in a Magnetically-Protected-First-Wall Laser Driven Reactor", Atomkernenergie (ATKE), 31, Lfg. 4, p. 217 (1978).
22. M.B. Emmett, "The MØRSE Monte Carlo Radiation Transport Code System", ORNL-4972, Oak Ridge National Laboratory (1975).
23. RSIC Code Package CCC-203, "MØRSE-CG", Radiation Shielding Information Center, ORNL (1976).
24. M.M.H. Ragheb and C.W. Maynard, "A Version of the MØRSE Multi-group Transport Code for Fusion Reactor Blankets and Shield Studies", BNL-20376, Brookhaven National Laboratory (1975).
25. B.E. Watt, "Energy Spectrum of Neutrons From Thermal Fission of U-235", Phys. Rev., 87, 1037 (1952).
26. D.M. Plaster, R.T. Santoro, and W.E. Ford III, "Coupled 100-Group Neutron and 21-Group Gamma-Ray Cross Sections for EPR Calculations", ORNL-TM-4872, Oak Ridge National Laboratory (1975).
27. W.E. Ford III, R.T. Santoro, R.W. Roussin, and D.M. Plaster, "Modification Number One to the Coupled 100 n - 21  $\gamma$  Cross Section Library for EPR Calculations", ORNL-TM-4259, Oak Ridge National Laboratory (1976).
28. DLC-37B Data Library, Radiation Shielding Information Center, Oak Ridge National Laboratory (1975).

29. G.D. Joanou and J.S. Dudek, "GAM II, A B3 Code for the Calculation of Fast Neutron Spectra and Associated Multi-group Constants", GA-4265, General Atomic (1973).
30. M.A. Abdou and R.W. Roussin, "MACKLIB, 100 Group Neutron Fluence-to-Kerma Factors and Reaction Cross Sections Generated by the MACK Computer Program From Data in ENDF Format", ORNL-TM-3995 (1974).
31. M.M.H. Ragheb and C.W. Maynard, "Statistical Weighting Monte Carlo Methods for External-Source-Driven Multiplying Media", UWFD-265, Univ. of Wisconsin (1978).
32. W.W. Engle, Jr., "A User's Manual for ANISN - A One-Dimensional Discrete Ordinate Code With Anisotropic Scattering", K-1693 (March 1967).
33. J.R. Lamarsh, "Introduction to Nuclear Reactor Theory", Addison-Wesley Publishing Company, p. 96 (1972).